

AD-A043 707

NAVAL WEAPONS SUPPORT CENTER CRANE IND
SENSITIVITY OF THE 'SHOE-BOX' IN P001 ANALYSIS, (U)
JUL 77 J L KEMP, N L PAPKE
NWSC/CR/RDTR-61

F/G 1/3

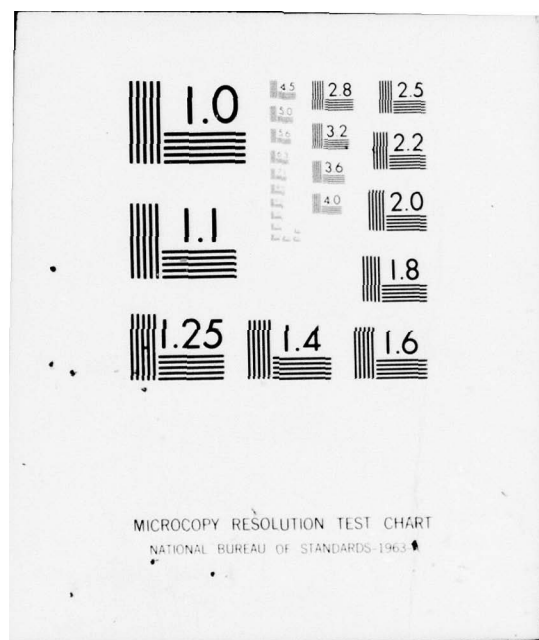
UNCLASSIFIED

NL

1 of 1
AD
A043707



END
DATE
FILMED
9-77
DDC



ADA043707

12
NW

NWSC/CR/RDTR-61

SENSITIVITY
OF
THE "SHOE-BOX" APPROACH
IN
POOL ANALYSIS

APPROVED FOR PUBLIC RELEASE
DISTRIBUTION UNLIMITED

JERRY KEMP
NORMAN PAPKE



PREPARED BY

APPLIED SCIENCES DEPARTMENT

NAVAL WEAPONS SUPPORT CENTER, CRANE, INDIANA

DDC FILE COPY

SECURITY CLASSIFICATION OF THIS PAGE (When Data Entered)

| REPORT DOCUMENTATION PAGE | | READ INSTRUCTIONS BEFORE COMPLETING FORM |
|---|-----------------------|---|
| 1. REPORT NUMBER NWSC/CR/RDTR-61 | 2. GOVT ACCESSION NO. | 3. RECIPIENT'S CATALOG NUMBER |
| 4. TITLE (and Subtitle) SENSITIVITY OF THE "SHOE-BOX" IN P001 ANALYSIS | | 5. TYPE OF REPORT & PERIOD COVERED |
| 7. AUTHOR(s) JERRY L. KEMP NORMAN L. PAPKE | | 6. PERFORMING ORG. REPORT NUMBER |
| 9. PERFORMING ORGANIZATION NAME AND ADDRESS Applied Sciences Department (502) Naval Weapons Support Center Crane, Indiana 47522 | | 8. CONTRACT OR GRANT NUMBER(s) IN-HOUSE |
| 11. CONTROLLING OFFICE NAME AND ADDRESS JTTCG/AS Central Office Naval Air Systems Command HQ (AIR-5204) Washington, D. C. 20361 | | 10. PROGRAM ELEMENT, PROJECT, TASK AREA & WORK UNIT NUMBERS TEAS 5.1.7.2 |
| 14. MONITORING AGENCY NAME & ADDRESS (if different from Controlling Office) Director Army Materials and Mechanics Research Center (AMXMR-MS, H. F. Campbell) Watertown, MA 02172 | | 12. REPORT DATE 11 23 Jul 1977 |
| 16. DISTRIBUTION STATEMENT (of this Report) Approved for Public Release; Distribution Unlimited | | 13. NUMBER OF PAGES 63 (1261p.) |
| 17. DISTRIBUTION STATEMENT (of the abstract entered in Block 20, if different from Report) | | 15. SECURITY CLASS. (of this report) UNCLASSIFIED |
| 18. SUPPLEMENTARY NOTES | | 15a. DECLASSIFICATION/DOWNGRADING SCHEDULE |
| 19. KEY WORDS (Continue on reverse side if necessary and identify by block number) Simulation; Artillery (AAA); Vulnerable Area; Presented Area; Probability of Hit; Probability of Kill; Survivability; Vulnerability; Bivariate Normal; Attrition Modeling | | |
| 20. ABSTRACT (Continue on reverse side if necessary and identify by block number) Survivability of aircraft against artillery threats can be assessed by a computer program, P001, which assumes that the vulnerable components are all centrally located on the aircraft. This report examines the sensitivity of this assumption and suggests a change to P001 to indicate when the assumption is not valid. | | |

DDC
SEP 1 1977
RECEIVED

DD FORM 1 JAN 73 1473

EDITION OF 1 NOV 65 IS OBSOLETE
S/N 0102-014-6601

UNCLASSIFIED

SECURITY CLASSIFICATION OF THIS PAGE (When Data Entered)

409351


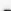
SECURITY CLASSIFICATION OF THIS PAGE(When Data Entered)



SECURITY CLASSIFICATION OF THIS PAGE(When Data Entered)

TABLE OF CONTENTS

| | <u>Page</u> |
|--|-------------|
| I. INTRODUCTION | 1 |
| II. POOL CONCEPTS | 2 |
| III. PROBABILITY OF HIT AT EXTREMITIES | 5 |
| IV. DESCRIPTION OF PARAMETERS. | 10 |
| V. EXAMPLE | 14 |
| VI. DISCUSSION OF RESULTS | 17 |
| VII. CONCLUSIONS | 20 |
| REFERENCES | 24 |
| APPENDIX A | A-1 |
| APPENDIX B | A-2 |

| | |
|---|---|
| The Section <input checked="" type="checkbox"/> | |
| & H Section <input type="checkbox"/> | |
| <input type="checkbox"/> | |
| DISCLOSURE AND ABUSE CODES | |
| OF SPECIAL | |
|  |  |

SENSITIVITY OF THE "SHOE-BOX" APPROACH IN P001 ANALYSIS

I. INTRODUCTION

One technique currently being widely used to assess the survivability of aircraft against artillery threats is the Anti-Aircraft Artillery Simulation Computer Program, AFATL Program P001 (reference (1)). P001 computes the single shot and cumulative probability of kill of a target aircraft flying a predefined flight path against a specific artillery threat. This is accomplished by computation of an aim point with consideration given to aiming errors, simulation of the firing process and its sources of error, combination of all the effects of random errors into one total trajectory distribution, location of the aircraft vulnerable area within this trajectory distribution, and, finally, computation of the probability of kill.

The aircraft vulnerable area data are calculated by other programs and entered into P001 in the form of a three-dimensional array as a function of relative projectile direction and relative striking velocity. In formulating vulnerable area tables, the aircraft's components that are vulnerable to a specific threat are established and their vulnerable areas are calculated. These component vulnerable areas are usually pooled in a "shoe-box" approach and assumed to be centrally located on the aircraft, even though some of the components may be located near the aircraft's extremities. This pooling of components introduces very small errors into the results

of P001 when the aircraft is small or the intercept range is long. However, when large aircraft or short ranges are involved, the probability of kill of a component (and the aircraft) can change significantly due to the component being located near the extremity rather than at the centroid. This change in probability of kill is actually due to a change in the probability of hit. These changes in probability of hit at different points on the aircraft can be quantitatively expressed using the bivariate normal distribution of projectile trajectories. The purpose of this report is to show these probability relationships and to suggest a change to P001 which will indicate when the shoe-box approach is not valid and when the distributed vulnerable area version of P001 should be used.

II. P001 CONCEPTS

The P001 Program methodology uses the concept of projectile dispersion about an aimpoint of the weapon. The distribution of projectiles is caused by random error, gun jitter, ballistic dispersion, atmospheric disturbance, flight roughness and muzzle velocity uncertainty. Systematic errors (bias), such as tracking lag, result in the projectile distribution being centered at an actual aimpoint of the weapon which does not coincide with the aircraft's center of gravity (centroid). (Note: The weapon is actually aimed at a point where the centroid is predicted to be at the time of intercept). The combination of all sources of random error considered in P001 is

assumed to result in a bivariate normal distribution of projectile trajectories. Terms used to describe this distribution are shown in Figure 1.

The orthogonal axes, f1 and f2, form a geometric plane which is the final coordinate system where the total projectile errors are axially independent. The coordinates of the position of the aircraft (considered as a point) with respect to the f1 and f2 axis are f1 bias and f2 bias. For the purposes of this analysis, the point (f1 bias, f2 bias) is considered to be the location of the centroid of the aircraft.

The standard deviations of the total projectile errors along the f1 and f2 axes are called s_{f1} and s_{f2} , respectively.

For ease of illustration, these two standard deviations were assumed equal in Figure 1. They will not generally be equal.

The geometric plane, f1-f2, is perpendicular to a line from the weapon to the point, (f1=0, f2=0). This point is the center of the projectile distribution. The ordinate, $g(f1, f2)$, of the bivariate normal at the point (f1, f2) is found using the following equation.

$$g(f1, f2) = (\exp (-1/2)[(f1/s_{f1})^2 + (f2/s_{f2})^2])/2\pi s_{f1}s_{f2}$$

The aircraft's centroid is located at (f1 bias, f2 bias) and $g(f1 \text{ bias}, f2 \text{ bias})$ is the ordinate of the bivariate normal at the centroid. P001 gives output values of f1 bias, f2 bias, s_{f1} and s_{f2} as a function of time. It also provides an output value for exposed vulnerable area (A_v) as a function of time. This value is calculated by linear interpolation from a 26-view table of vulnerable

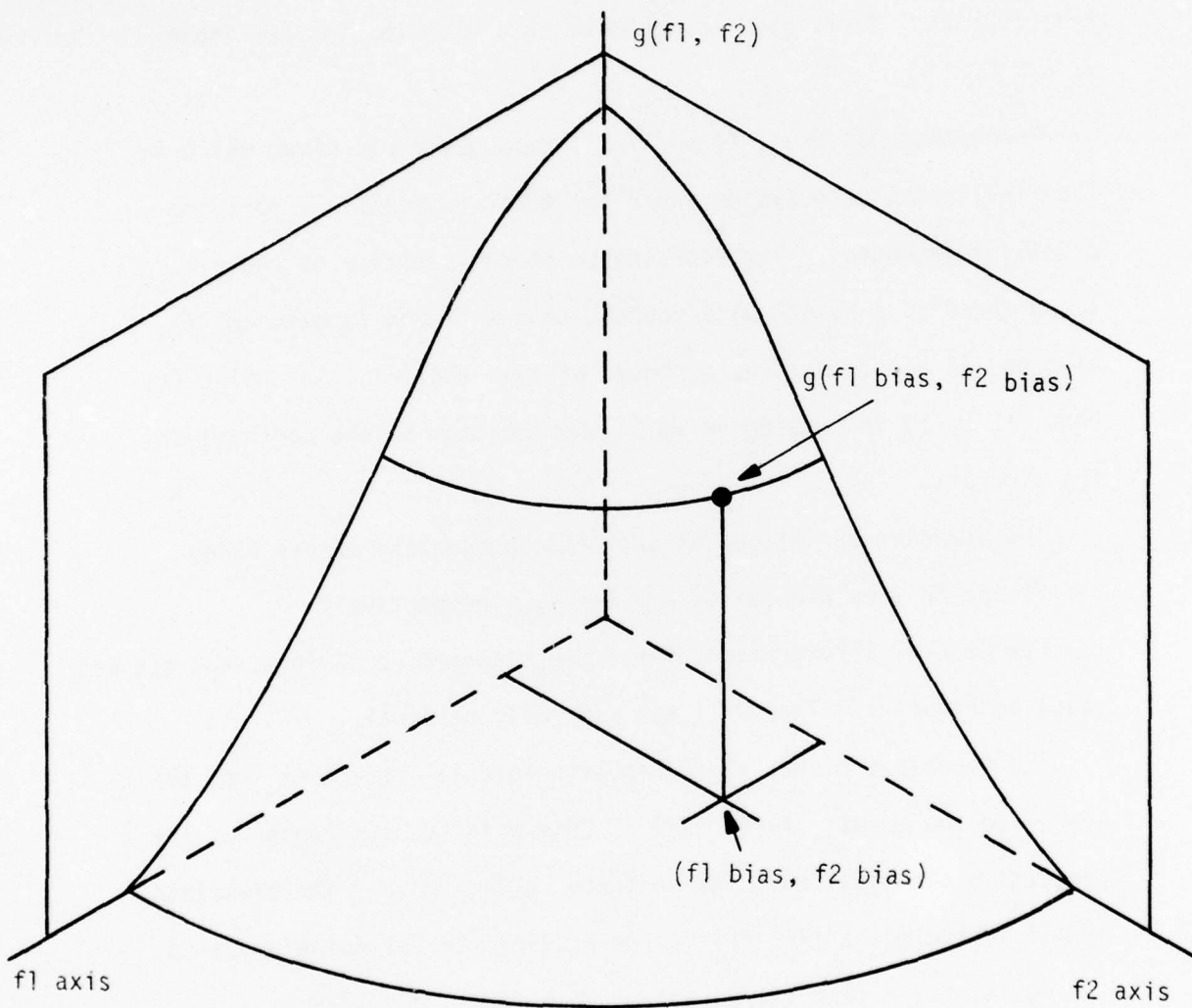


FIGURE 1
BIVARIATE NORMAL DISTRIBUTION OF PROJECTILES

areas for the appropriate geometric relation between projectile and aircraft. If presented areas (A_p) are used in the 26-view table instead of A_v , the computer output value labeled A_p will be the "exposed" presented area for each set of geometric positions, and the value labeled P_k is the probability of hit.

III. PROBABILITY OF HIT AT CENTROID

A mathematical approach was taken to determine the sensitivity of P001 to the shoe-box assumption. The parameters of the bivariate normal distribution ($f1$ bias, $f2$ bias, s_{f1} , s_{f2}) and the presented area were obtained from P001 computer runs. Those parameters were then used to determine the probability of hit at an extremity point relative to the probability of hit at the centroid (see Figure 2). If the probability of hit at an extremity is significantly different from the probability of hit at the centroid, each vulnerable component that is located at an extremity should be analyzed separately using the techniques shown in reference (2). If there are no significant probability differences, the methodology which assumes equally likely hits throughout the presented area of the aircraft, i.e., the shoe-box approach, is acceptable.

To calculate the probability of hit, it is convenient to define an arbitrarily small area, ΔA , which is small enough to consider $g(f1, f2)$ constant for all points ($f1, f2$) contained in ΔA . Consider ΔA as much smaller than A_p .

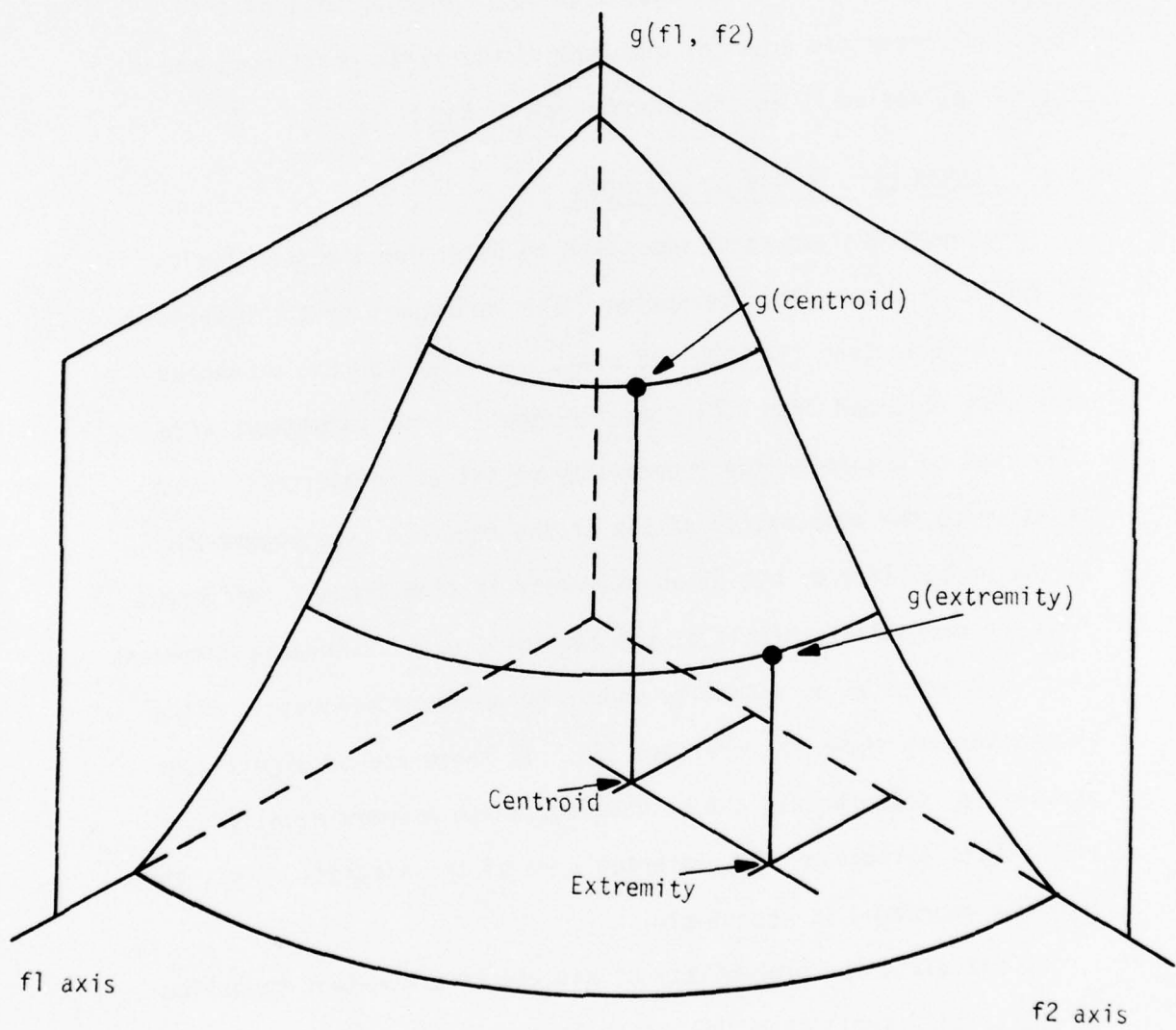


FIGURE 2
BIVARIATE NORMAL, DEPICTING
 $g(\text{CENTROID})$ AND $g(\text{EXTREMITY})$

$$P(\text{hit on } \Delta A) = \iint_{\Delta A} g(f_1, f_2) df_1 df_2$$

located at
f1, f2

= $\Delta A \cdot g(f_1, f_2)$ This represents the volume of a cylinder whose base has an area of ΔA and whose height is $g(f_1, f_2)$. Based on the above equation, the ratio of the probabilities of hit at the centroid and an extremity is expressed as follows:

$$\begin{aligned} \text{Ratio} &= \frac{P(\text{Hit on } \Delta A \text{ at Centroid})}{P(\text{Hit on } \Delta A \text{ at Extremity})} = \frac{\Delta A \cdot g(\text{centroid})}{\Delta A \cdot g(\text{extremity})} \\ &= \frac{g(\text{centroid})}{g(\text{extremity})} \end{aligned}$$

To conduct this analysis, some simplifying assumptions were made regarding the locations of the extremities of an aircraft relative to its centroid. The presented area was considered to be a rectangle, with the centroid in the center and the extremities located at the midpoints of the four sides. The rectangle was defined as shown below.

A_p exposed = $l' \times h'$, where

A_p exposed = exposed presented area of the aircraft,

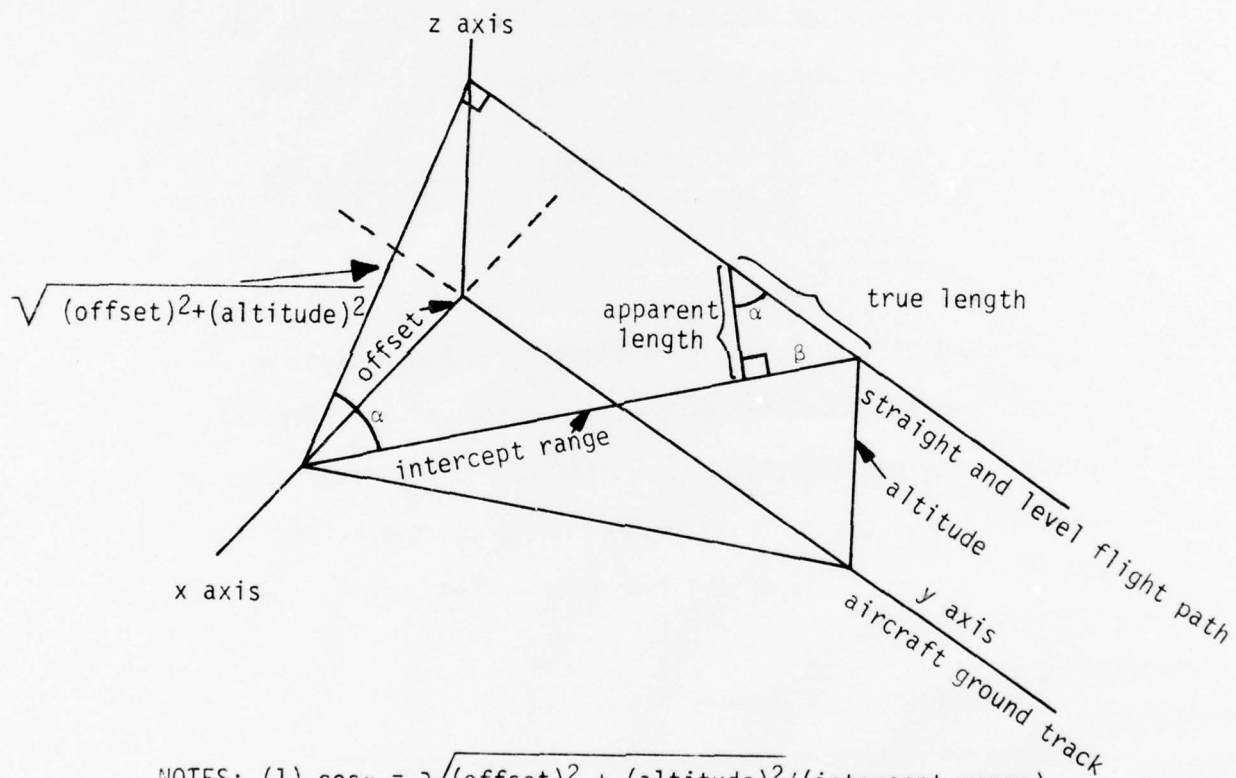
l' = apparent length of the aircraft, and

h' = apparent height of the aircraft.

The apparent length (l') of the aircraft was computed as follows:

$$l' = \text{true length} \sqrt{(\text{offset})^2 + (\text{altitude})^2} / (\text{intercept range})$$

The apparent height (h') was then calculated by dividing the "exposed" presented area by the apparent length. The geometry of the apparent length is shown in Figure 3



- NOTES: (1) $\cos \alpha = \frac{\sqrt{(\text{offset})^2 + (\text{altitude})^2}}{(\text{intercept range})}$
 (2) $\text{apparent length} = (\text{true length}) \cos \alpha$
 $= (\text{true length}) \frac{\sqrt{(\text{offset})^2 + (\text{altitude})^2}}{(\text{intercept range})}$

FIGURE 3
 GEOMETRY OF APPARENT LENGTH OF AIRCRAFT

The five ordinates of the bivariate normal distribution (representing the centroid and four extremities) which were used in this analysis are shown below.

$$g(\text{centroid}) = g(f1 \text{ bias}, f2 \text{ bias})$$

For the extremities, as pictured in Figure 4, the ordinates are as follows:

$$g(\text{extremity 1}) = g(f1 \text{ bias} + .5(l'), f2 \text{ bias})$$

$$g(\text{extremity 2}) = g(f1 \text{ bias} - .5(l'), f2 \text{ bias})$$

$$g(\text{extremity 3}) = g(f1 \text{ bias}, f2 \text{ bias} + .5h')$$

$$g(\text{extremity 4}) = g(f1 \text{ bias}, f2 \text{ bias} - .5h')$$

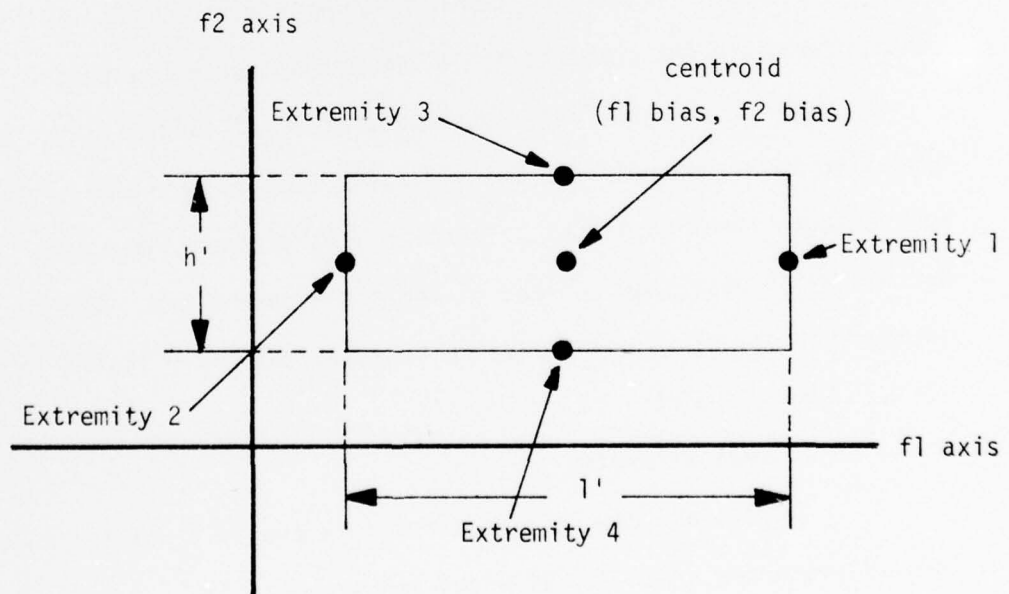


FIGURE 4
RELATIVE LOCATION OF CENTROID AND FOUR EXTREMITIES
IN f1-f2 COORDINATE SYSTEM

The maximum of the set of ratios,

$$\frac{g(\text{centroid})}{g(\text{extremity 1})}, \frac{g(\text{centroid})}{g(\text{extremity 2})}, \frac{g(\text{centroid})}{g(\text{extremity 3})}, \frac{g(\text{centroid})}{g(\text{extremity 4})}$$

was used as an indicator of the severity of the problems resulting from the shoe-box concept for that set of encounter conditions.

IV. DESCRIPTION OF PARAMETERS

The input parameters of the model were varied to investigate the sensitivity of the model to the assumption that all vulnerable components are located at the aircraft's centroid. The ranges of input values were selected to ensure that examples are shown for conditions where the assumptions are met and where the assumptions are not met. The reader can then develop an understanding of the conditions where the constraints of the assumption are exceeded.

The analysis was performed using two sizes of aircraft, two weapon-operating mode combinations, two aircraft velocity-altitude combinations, and various offset distances. Fourteen sets of input data were defined which were combinations of the above parameters. The parameters are further described below and the fourteen cases are listed in Table 1.

A. Aircraft Size

1. Small aircraft

The small aircraft used for this analysis was the A-7. The A-7 presented areas for 26-views are shown in Table A-1 of the Appendix. These 26-views are defined on page 2-15 of Volume I of

TABLE 1
DEFINITION OF PARAMETERS FOR SCENARIOS
USED IN THE ANALYSIS (14 SETS OF CONDITIONS)

| CASE | WEAPON | | AIRCRAFT | | | OFFSET | FIGURE | TABLES |
|------|--------|------|-------------|----------|----------|--------|--------|--------|
| | TYPE | MODE | COMMENT | VELOCITY | ALTITUDE | | | |
| 1 | 2 | 1 | Low-Slow | 50 | 75 | 100 | A-1 | A-2 |
| 2 | 2 | 1 | Low-Slow | 50 | 75 | 200 | A-2 | A-3 |
| 3 | 2 | 1 | Low-Slow | 50 | 75 | 500 | A-3 | A-4 |
| 4 | 2 | 1 | Fast-Higher | 250 | 500 | 100 | A-4 | A-5 |
| 5 | 2 | 1 | Fast-Higher | 250 | 500 | 200 | A-5 | A-6 |
| 6 | 2 | 1 | Fast-Higher | 250 | 500 | 500 | A-6 | A-7 |
| 7 | 3A | 2 | Low-Slow | 50 | 75 | 200 | A-7 | A-8 |
| 8 | 3A | 2 | Low-Slow | 50 | 75 | 500 | A-8 | A-9 |
| 9 | 3A | 2 | Low-Slow | 50 | 75 | 1000 | A-9 | A-10 |
| 10 | 3A | 2 | Low-Slow | 50 | 75 | 2500 | A-10 | A-11 |
| 11 | 3A | 2 | Fast-Higher | 250 | 500 | 200 | A-11 | A-12 |
| 12 | 3A | 2 | Fast-Higher | 250 | 500 | 500 | A-12 | A-13 |
| 13 | 3A | 2 | Fast-Higher | 250 | 500 | 1000 | A-13 | A-14 |
| 14 | 3A | 2 | Fast-Higher | 250 | 500 | 2500 | A-14 | A-15 |

reference (1). The length (13.7 meters) of the A-7 was obtained by scaling the drawings in reference (3). The left side view of the drawings is the same aspect as view 16 (270° longitude, 90° latitude) of the 26-view set. From Table A-1 of the Appendix the presented area from view 16 is 31.55 square meters. Therefore, the A-7 from this aspect is considered to be a rectangle with a length of 13.7 meters and a height of 2.3 meters.

The A-7 dimensions are close enough to the A-10 dimensions so that any conclusions reached relative to the A-7 as a small aircraft would also be applicable to the A-10.

2. Large Aircraft

The large aircraft for this analysis was defined as a transport aircraft whose dimensions were approximately twice as long and twice as high as those of the A-7. The C-130 (see reference (3)) and YC-14 transports fit into this size category.

B. Aircraft Velocity - Altitude

Two combinations of aircraft velocity and altitude were used in the analysis. The low and slow combination of 50 meters/sec velocity and an altitude of 75 meters was used to represent operations involving the A-10 and large transport aircraft. The combination of 250 meters/sec at an altitude of 500 meters was used since this is typical of A-7 and some transport operations.

C. Weapon Types and Modes

The threat weapons and operating modes in this analysis were weapon type 2 operating in mode 1 and weapon type 3A operating in mode 2. The definitions of these codes can be found in reference (4). These weapon threats are realistic for operations involving the A-7 A-10, and the tactical transport aircraft.

D. Offset Distance

The offset distance is defined as the distance from the weapon to the point of closest approach on the aircraft's ground track. Three values of offset distance were used for weapon 2 mode 1. These values were 100, 200 and 500 meters. Due to the inherent limitations of mode 1 operation, offset distances greater than 500 meters were not used for fast aircraft because very few projectiles can be fired for this situation.

Four values of offset distance were used for weapon 3A mode 2. These values were 200, 500, 1000, and 2500 meters. The projectile flight time limit for weapon 3A mode 2 is 7.5 seconds, which limits intercept range to roughly 3000 meters. Offset distances larger than 2500 meters and less than 3000 meters would allow very little firing data.

V. CALCULATION EXAMPLE

An example of the calculation of the probability of hit at the centroid versus the probability of hit at an extremity will be shown in this section. This example uses the small aircraft (A-7 size) at the conditions of Case 7 of Table 1. The input values for the P001 computer runs for this example are shown in Table 2 below.

TABLE 2
PARAMETERS OF THE EXAMPLE

| <u>Parameter</u> | <u>Value Assigned</u> |
|--|-----------------------|
| Threat Weapon | Weapon 3A, Mode 2* |
| Aircraft Altitude | 75 Meters |
| Aircraft Velocity | 50 Meters/Second |
| Offset (distance from weapon to point of closest approach of ground track of the aircraft) | 200 Meters |
| Presented Areas (26 views) | See Appendix A |
| Aircraft Flight Path | Straight and Level |

* Refer to reference (4) for description

The values used for this probability example (see Table 3) were taken from a typical line of P001 output (one firing time step).

TABLE 3
P001 OUTPUT PARAMETERS FOR THE EXAMPLE

| <u>Parameter</u> | <u>Value</u> |
|--|---------------------|
| Intercept Range | 505 meters |
| s_{f1} | 3.6 meters |
| s_{f2} | 3.5 meters |
| f1 bias | 0.1 meters |
| f2 bias | 0.4 meters |
| "Exposed" Presented Area (print-out label - vulnerable area) | 19.85 square meters |

The true length from reference (3), of the A-7 is 13.7 meters. The apparent length (l') is calculated below.

$$\begin{aligned}
 l' &= (\text{true length}) \sqrt{(\text{offset})^2 + (\text{altitude})^2} / (\text{Intercept Range}) \\
 &= (13.7) \sqrt{200^2 + 75^2} / 505 \\
 &= 5.8 \text{ meters}
 \end{aligned}$$

Since the exposed presented area of this rectangle in space is the product of its apparent length and apparent height (h'),

$$\begin{aligned}
 h &= \text{"exposed" presented area} / \text{apparent length} \\
 &= 19.85 / 5.8 \\
 &= 3.4 \text{ meters}
 \end{aligned}$$

Using these values of apparent length and height, the extremities are shown in Figure 5.

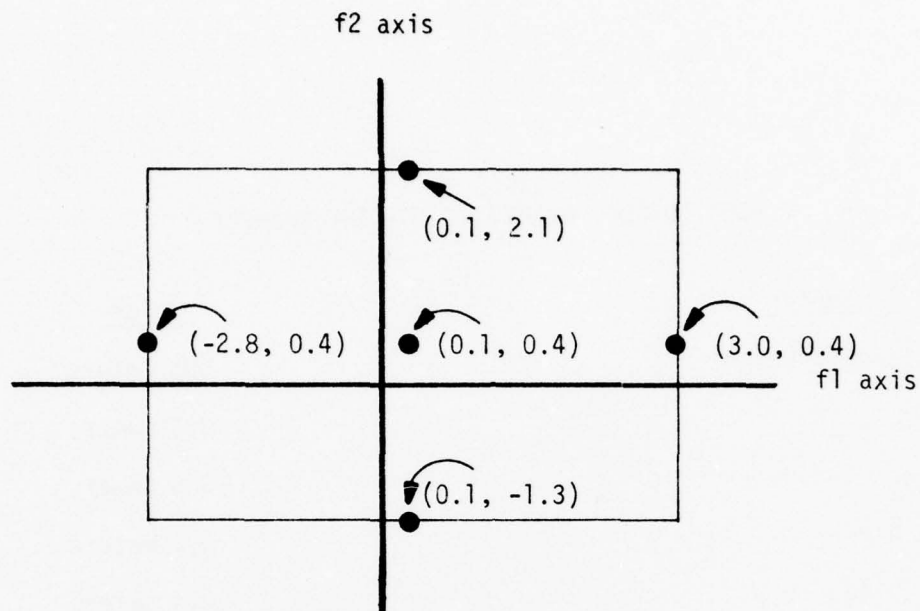


FIGURE 5 - LOCATIONS OF CENTROID AND EXTREMITIES FOR THE EXAMPLE

The values for calculating the ratios of probability of hit are shown below. (The equation for the ordinate, $g(f1, f2)$, of the bivariate normal was given in Section II.)

$$g(\text{centroid}) = g(0.1, 0.4) = .0125$$

Extremities

$$g(3.0, 0.4) = .0089$$

$$g(-2.8, 0.4) = .0093$$

$$g(0.1, 2.1) = .0105$$

$$g(0.1, -1.3) = .0118$$

$$\text{Maximum Ratio} = \frac{.0125}{.0089} = 1.4$$

This value of 1.4 shows that the centroid (0.1, 0.4) is 40% more likely to be hit than the extremity, (3.0, 0.4).

VI. DISCUSSION OF RESULTS

The results from the 14 cases described in Table 1 are graphically shown in appendix as Figures A-1 through A-14. The specific data points for these graphs are shown in the appendix as Tables A-2 through A-15. Figure A-1 of the appendix is also presented as Figure 6 of the report body for explanation of concepts and terms.

The minimum possible intercept range shown in the graphs is computed as shown below (Figure 3 shows the geometry for this distance).

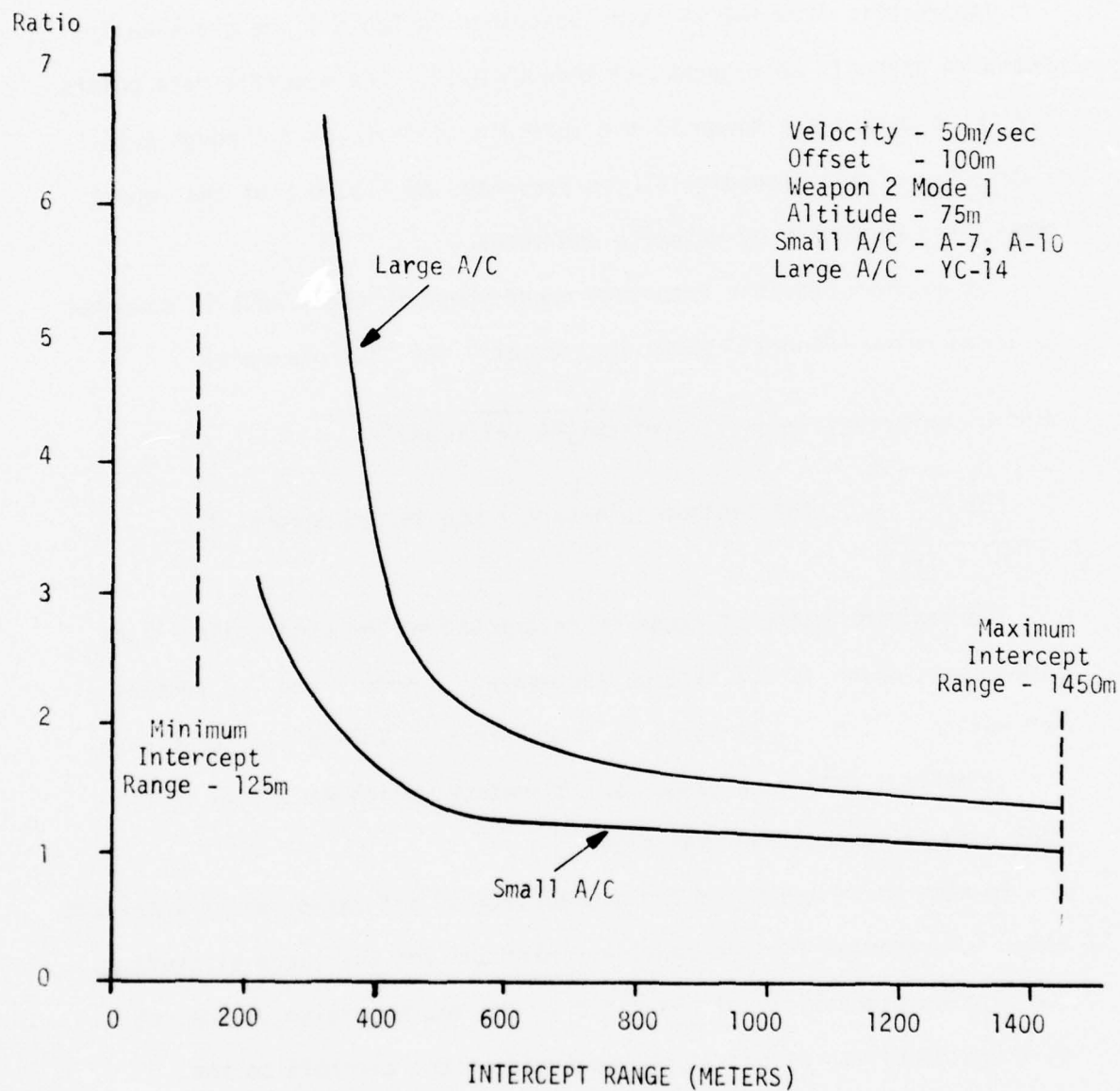
$$\text{Minimum Intercept Range} = \sqrt{(\text{offset})^2 + (\text{altitude})^2}$$

For Figure 6, the minimum intercept range is 125 meters, i.e., $\sqrt{(100^2 + 75^2)}$.

The maximum intercept range is restricted by the projectile flight time limit, which is 2.2 seconds for weapon 2 mode 1 and 7.5 seconds for weapon 3A mode 2, as shown in reference (1), Volume I. For Figure 6, the maximum intercept range is 1450 meters, which was shown in the P001 computer output for that case.

On each graph a plot of the probability of hit ratio versus intercept range is presented for the small aircraft and for the large aircraft. The plotted probability of hit ratio is the maximum value of the ratios of the probability of hit at the centroid of the aircraft to the probability of hit at each of the four extremities (see the earlier discussion in Section III). The ratios for the large aircraft are always larger than the ratios for the small aircraft since

PROBABILITY OF HIT RATIO* VERSUS
INTERCEPT RANGE - SLOW A/C



*Ratio of P_H (centroid) to P_H (extremity)

FIGURE 6

the extremities of the large aircraft extend further into the tails of the bivariate normal distribution.

In Figure 6, a ratio of 3.0 occurs at a range of approximately 450 meters for the large aircraft and 250 meters for the small aircraft. As the ranges decrease from these points the ratios increase rapidly. Even though the curves are relatively flat for intercept ranges greater than 800 meters, the large aircraft's ratio remains above 1.4 for all ranges. Figure 6 also shows a divergence between the curves as intercept range decreases, with the slope of the large aircraft's curve being steeper. Since it is also true that the ratio is higher for the large aircraft than for the small over all ranges, the large aircraft is more sensitive than the small aircraft to the shoe-box assumption.

One of the data points selected for discussion from Figure 6 shows a ratio of 1.5 for the large aircraft at an intercept range of 800 meters. A ratio of 1.5 means that the probability of hit at the centroid is 50% greater than the probability of hit at the extremity. The small aircraft has a ratio of 1.5 at an intercept range of 420 meters. Thus, the small aircraft does not reach the 50% greater probability of hit point until the intercept range decreases to 420 meters.

In order to summarize the results shown graphically in Figures A-1 through A-14, the following categories of effects of the shoe-

box approach were established:

(1) Category A - Over some interval of intercept ranges, the ratio exceeds 3.0.

(2) Category B - The maximum ratio for any intercept range is less than 3.0 but greater than 1.5.

(3) Category C - For all intercept ranges, the ratio does not exceed 1.5.

The placement of the various cases into these three categories is shown in Table 4.

In general, the most sensitive (Category A) cases were those in which the aircraft was flying low and slow and/or at small offset distances. For weapon type 2, this included all cases in which the aircraft was flying low and slow, except the small aircraft at the maximum offset distance used (500 meters). For weapon type 3A, Category A cases included the fast and higher aircraft at close range (200 meters offset), as well as the low and slow aircraft for all offset distances except 2500 meters. Seven of the fourteen sets of conditions for the large aircraft and five of fourteen for the small aircraft were in Category A.

VIII. CONCLUSIONS

Since the analysis has shown that situations can exist in which the results are sensitive to the shoe-box assumption, it is recommended

TABLE 4
CLASSIFICATION OF THE VARIOUS CASES
INTO CATEGORIES OF SENSITIVITY

| Category | Case | Weapon | | Aircraft | | |
|----------|------|--------|--------------|----------|------|----------------|
| | | Type | Offset Dist. | Vel. | Alt. | Large or Small |
| A | 1 | 2 | 100 | 50 | 75 | L,S |
| | 2 | 2 | 200 | 50 | 75 | L,S |
| | 3 | 2 | 500 | 50 | 75 | L |
| | 7 | 3A | 200 | 50 | 75 | L,S |
| | 8 | 3A | 500 | 50 | 75 | L,S |
| | 9 | 3A | 1000 | 50 | 75 | L |
| | 11 | 3A | 200 | 250 | 500 | L,S |
| B | 3 | 2 | 500 | 50 | 75 | S |
| | 9 | 3A | 1000 | 50 | 75 | S |
| | 12 | 3A | 500 | 250 | 500 | L |
| | 13 | 3A | 1000 | 250 | 500 | L |
| C | 4 | 2 | 100 | 250 | 500 | L,S |
| | 5 | 2 | 200 | 250 | 500 | L,S |
| | 6 | 2 | 500 | 250 | 500 | L,S |
| | 10 | 3A | 2500 | 50 | 75 | L,S |
| | 12 | 3A | 500 | 250 | 500 | S |
| | 13 | 3A | 1000 | 250 | 500 | S |
| | 14 | 3A | 2500 | 250 | 500 | L,S |

that P001 be modified to identify each computer run as sensitive or insensitive to the shoe-box assumption. The decision regarding sensitivity would be based on the probability of hit ratios between the centroid and extremities. Only the front and rear extremities need to be considered since, in all the cases investigated in this study, the maximum ratio occurred at one of the extremities along the longitudinal axis.

This modification would involve describing the positions of the front and rear extremities relative to the centroid, projecting those locations onto the f1-f2 plane at each time step (as shown in reference (2)), and computing ratios of probabilities of hit for the centroid and extremities by using the ordinates of the bivariate normal at the three points (as described in Section II). Each line of the shot history output of P001 would contain an additional parameter, which would be the maximum of the two ratios,

$$\frac{g(\text{centroid})}{g(\text{front extremity})} \quad \text{and} \quad \frac{g(\text{centroid})}{g(\text{rear extremity})}.$$

The analyst would then decide whether the value of this parameter varies enough from the expected value of 1.0 over the course of the shot history to warrant the use of more lengthy procedures which require the specific location of each vulnerable component (described in reference (2)).

In this recommended modification, presented area tables would not be required in the computation. The presented area tables were used in this report to approximate possible extreme locations for vulnerable components.

The technique for determining the exact position of a vulnerable component (not at the centroid) in the f_1 - f_2 geometric plane as shown in reference (2) is summarized in Appendix B.

REFERENCES

1. James Severson, Thomas McMurchie, *Anti-Aircraft Artillery Simulator Computer Program - AFATL Program P001*, Naval Weapons Center, China Lake, CA, September 1973
2. *P001 Computer Program Update*, Armament Systems Inc., Anaheim, CA April 1976.
3. *Jane's All the World's Aircraft*, McGraw-Hill, 1972-1973
4. James Severson, Thomas McMurchie, *Documentation of Anti-Aircraft Artillery Simulation Computer Program -- AFATL Program P001 (U)*, SECRET, Air Force Armament Lab., Elgin Air Force Base, FL, Armament Memorandum Report 72-3, March 1972

APPENDIX A

FIGURES A-1 through A-14

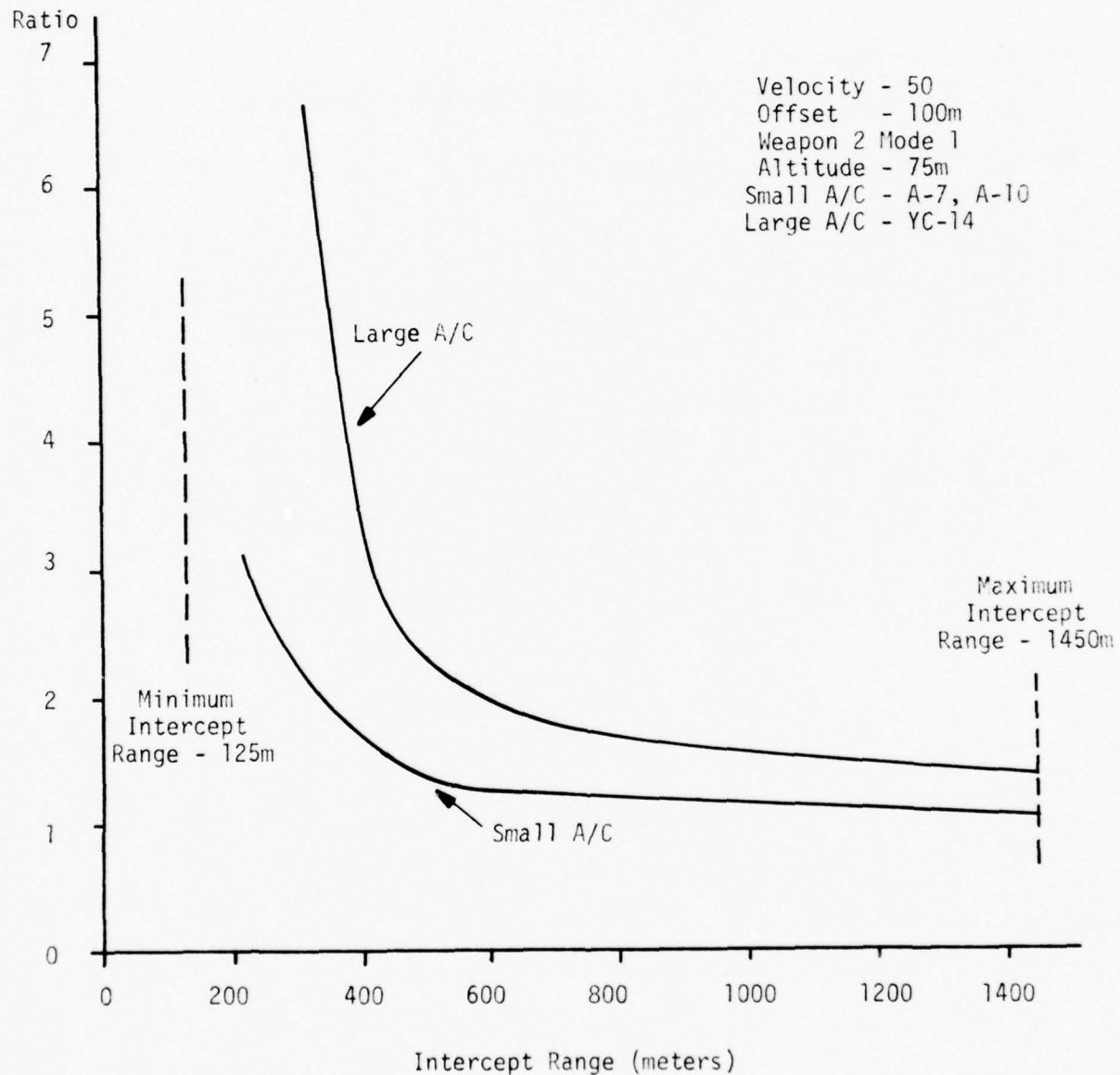
Probability of Hit Ratio versus Intercept Range for each of
14 Scenario Conditions

TABLE A-1 Presented areas for the A-7 (26-views)

TABLES A-2 through A-15

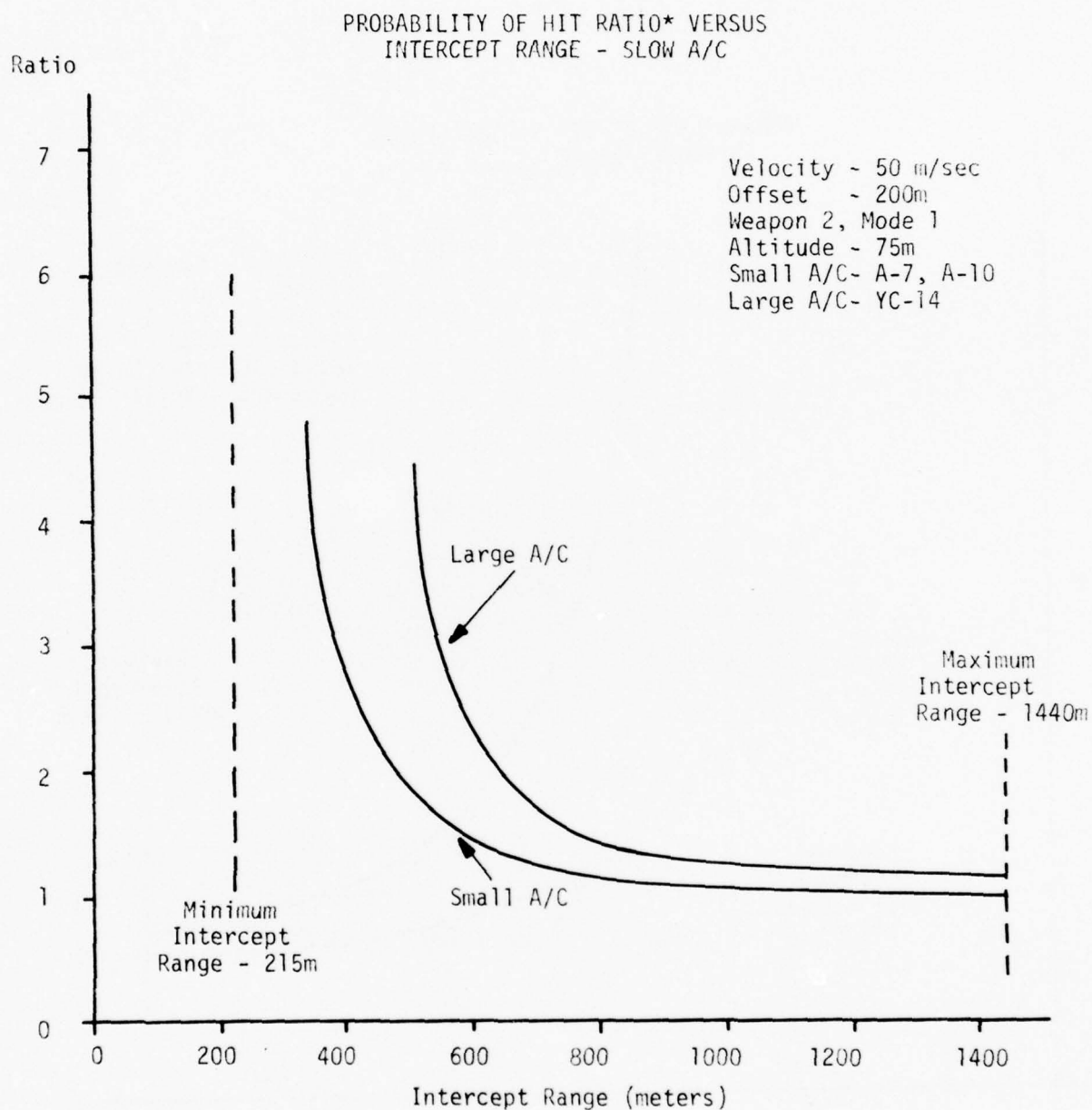
Tables of Data; S_{f1} , S_{f2} , f1 bias, f2 bias, l'/h' , "Exposed"
Presented Areas for Large and Small Aircraft, and Probability
of Hit Ratios Versus Intercept Range for Each of 14 Scenario
Conditions

PROBABILITY OF HIT RATIO* VERSUS
INTERCEPT RANGE - SLOW A/C



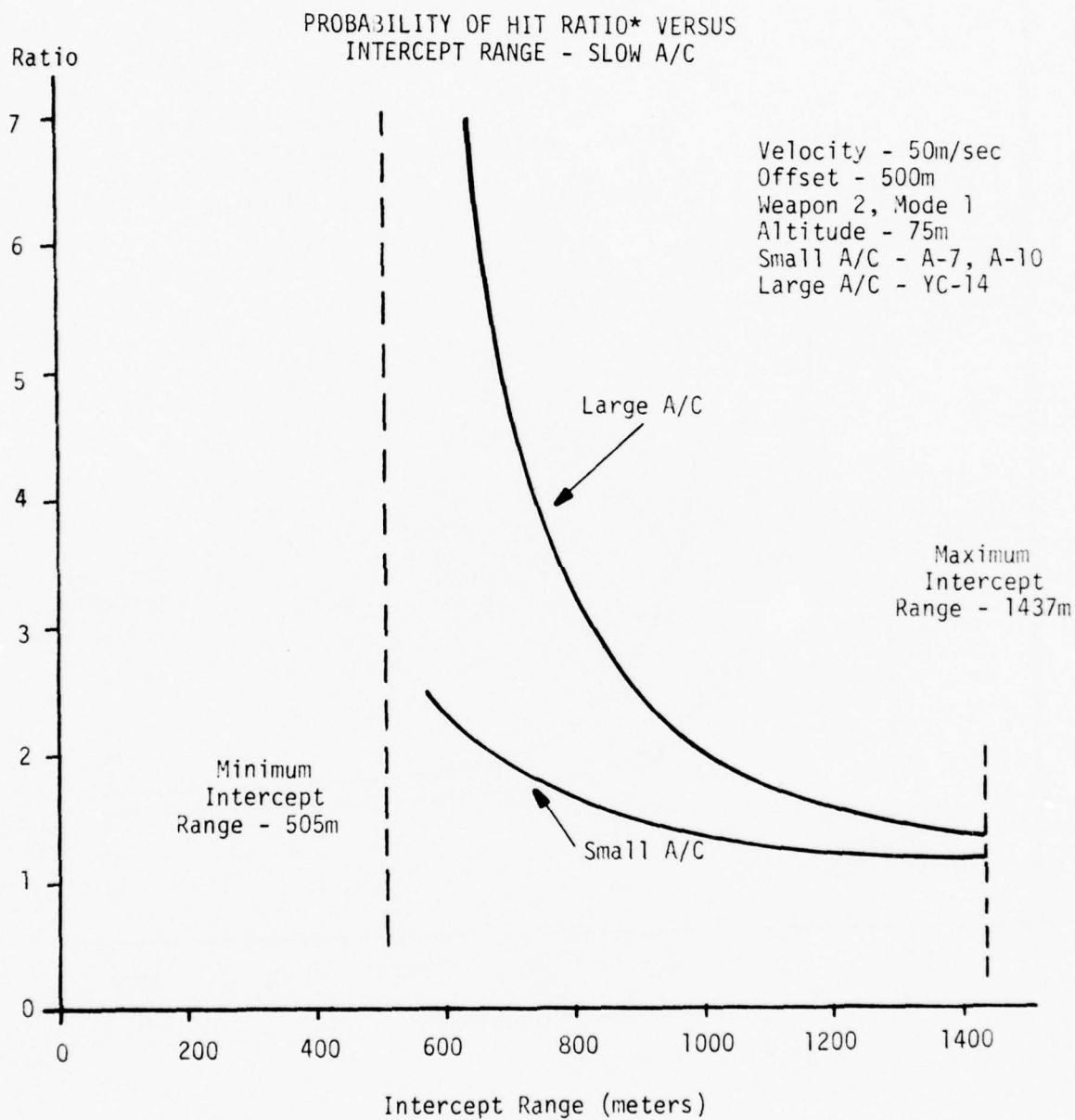
* Ratio of P_H (centroid) to P_H (extremity)

FIGURE A-1



*Ratio of P_H (centroid) to P_H (extremity)

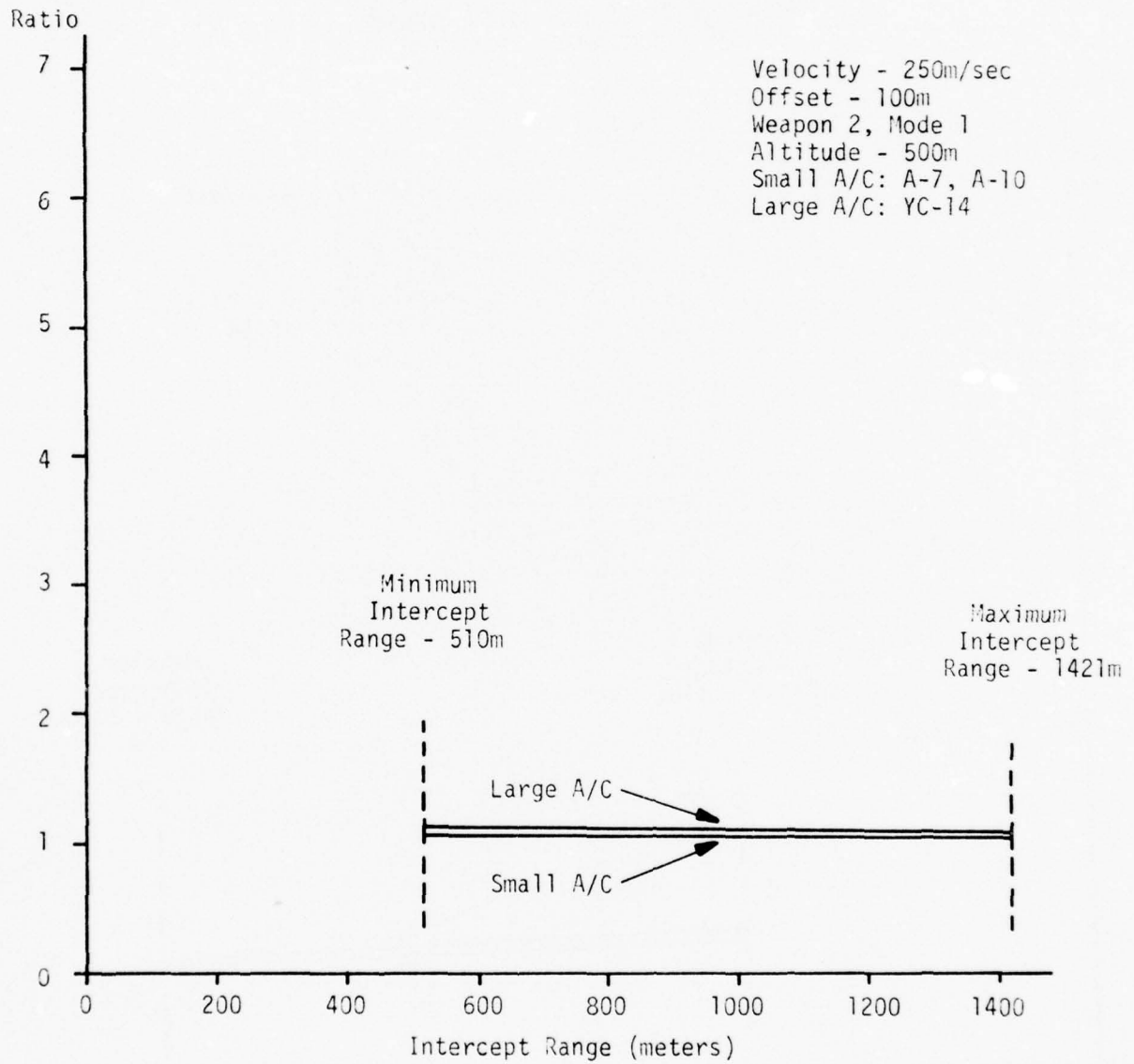
FIGURE A-2



*Ratio of P_H (centroid) to P_H (extremity)

FIGURE A-3

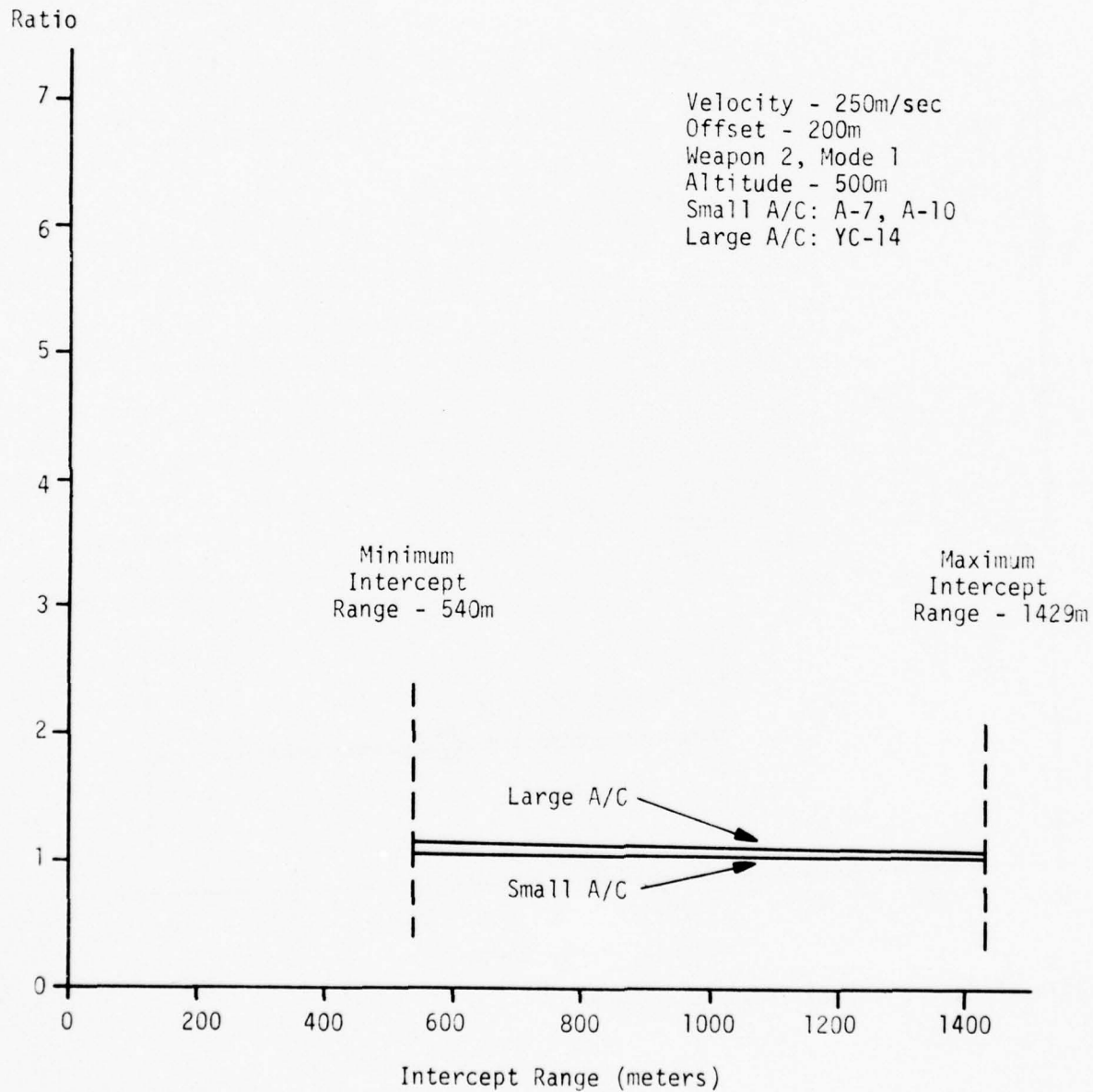
PROBABILITY OF HIT RATIO* VERSUS
INTERCEPT RANGE - FAST A/C



*Ratio of P_H (centroid) to P_H (extremity)

FIGURE A-4

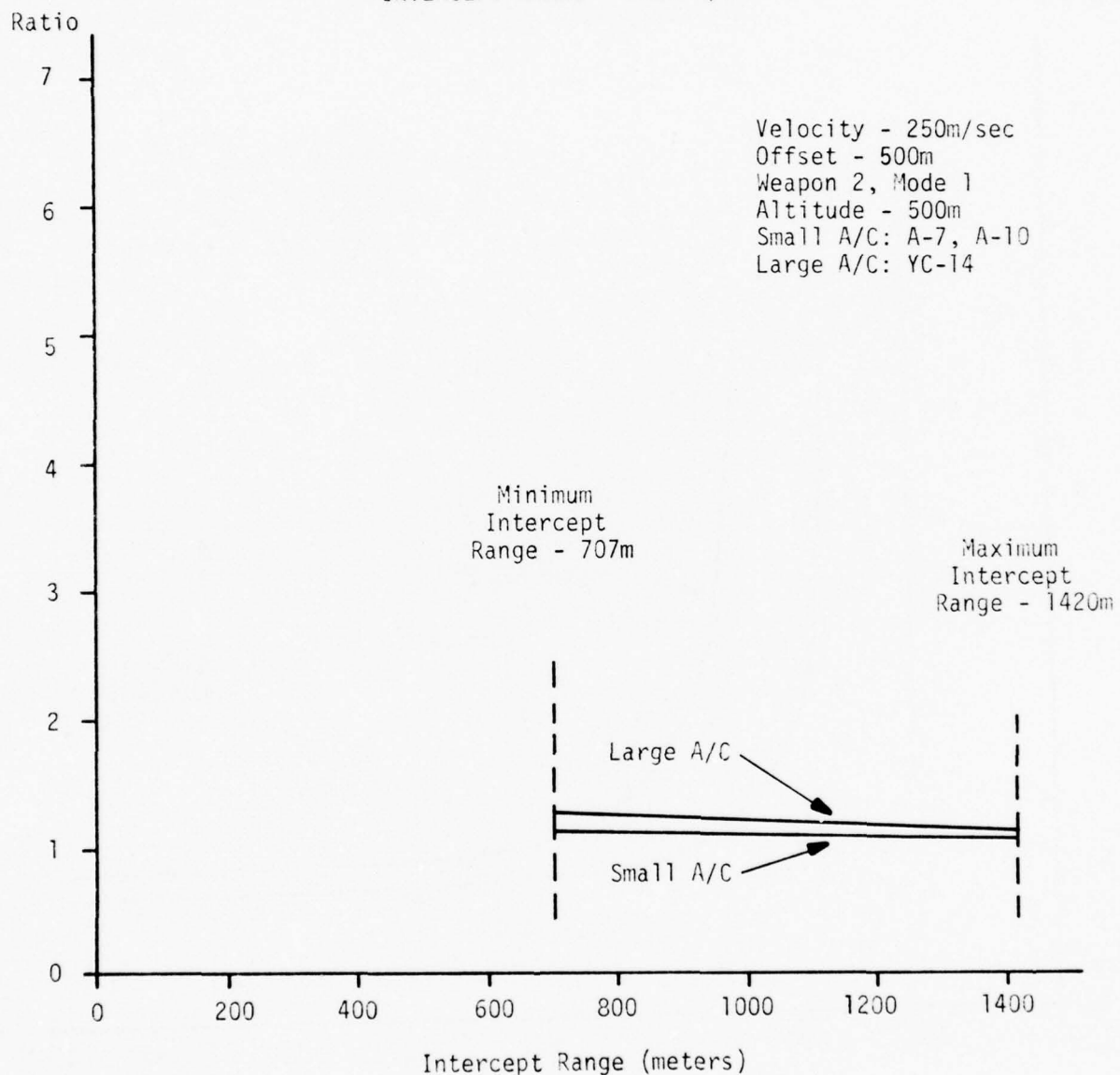
PROBABILITY OF HIT RATIO* VERSUS
INTERCEPT RANGE - FAST A/C



*Ratio of P_H (centroid) to P_H (extremity)

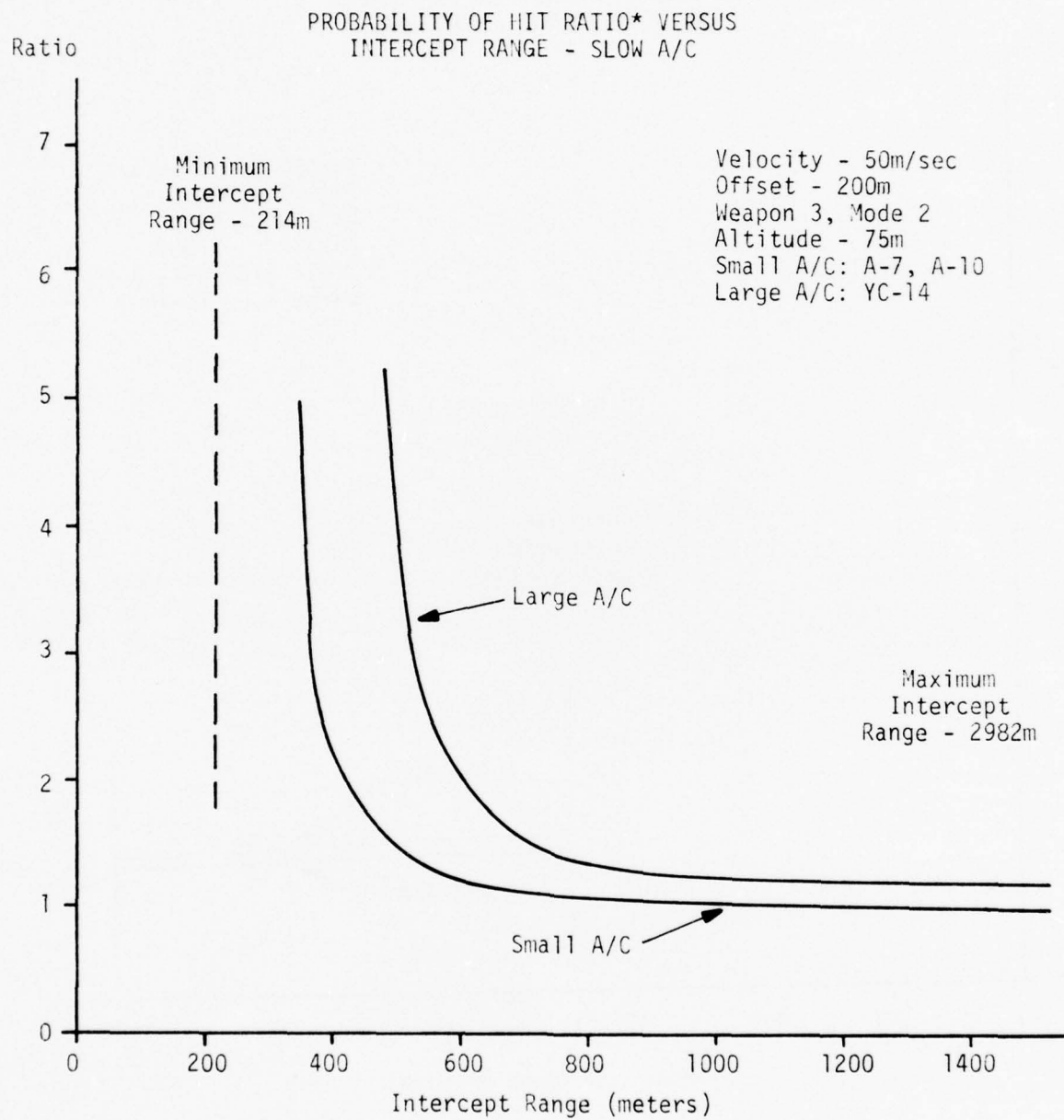
FIGURE A-5

PROBABILITY OF HIT RATIO* VERSUS
INTERCEPT RANGE - FAST A/C



*Ratio of P_H (centroid) to P_H (extremity)

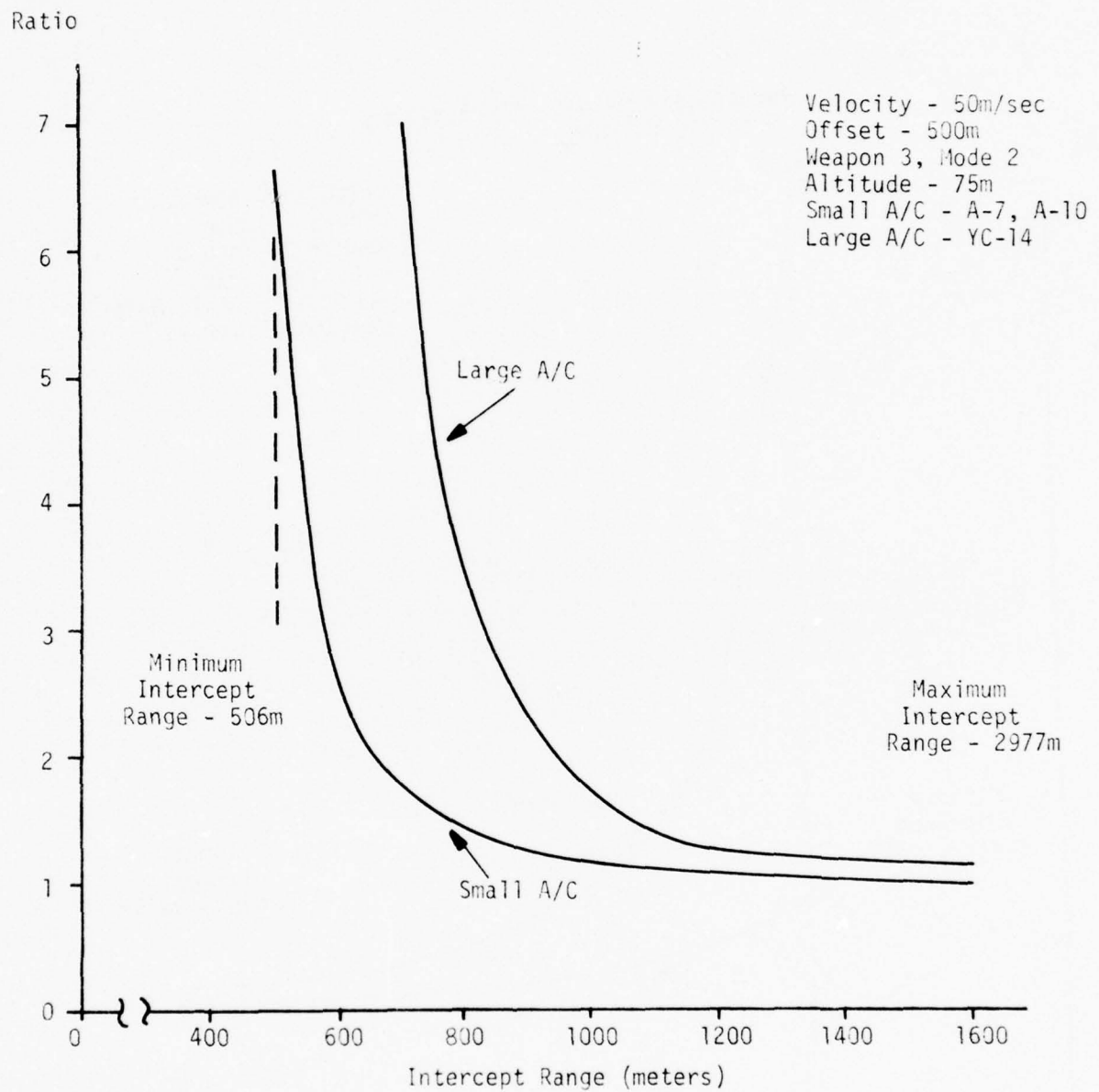
FIGURE A-6



*Ratio of P_H (centroid) to P_H (extremity)

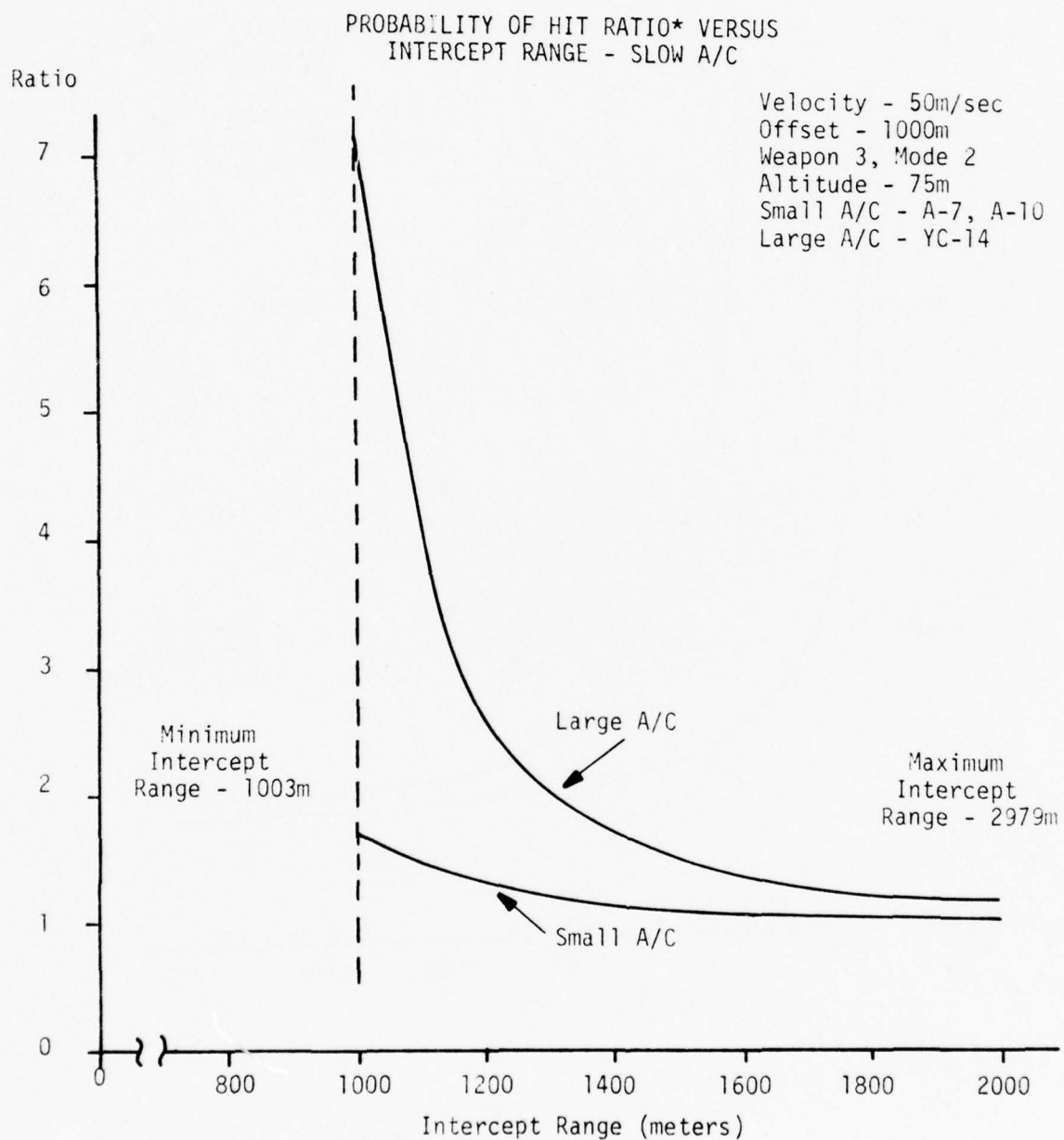
FIGURE A-7

PROBABILITY OF HIT RATIO* VERSUS
INTERCEPT RANGE - SLOW A/C



*Ratio of P_H (centroid) to P_H (extremity)

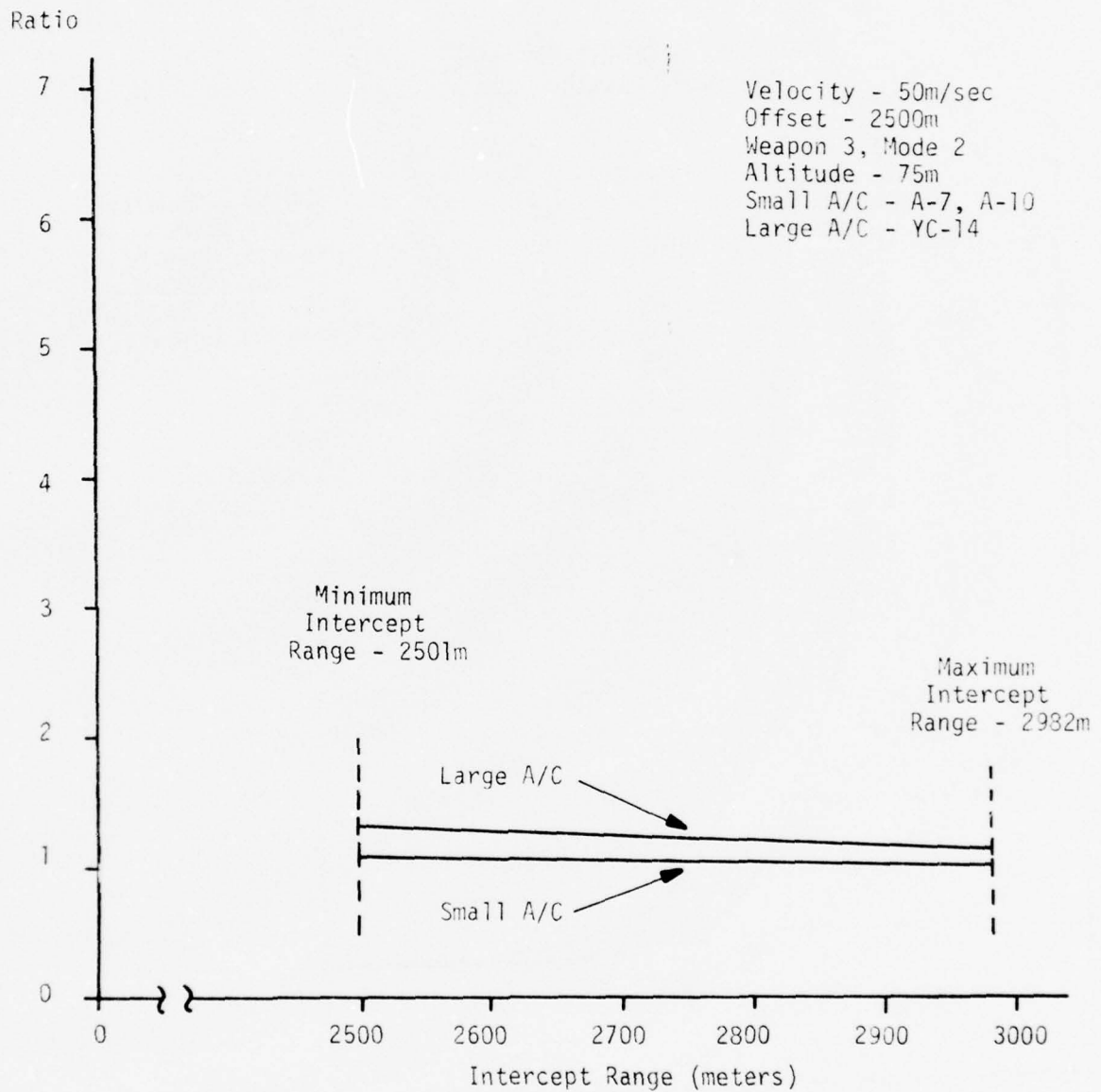
FIGURE A-8



*Ratio of P_H (centroid) to P_H (extremity)

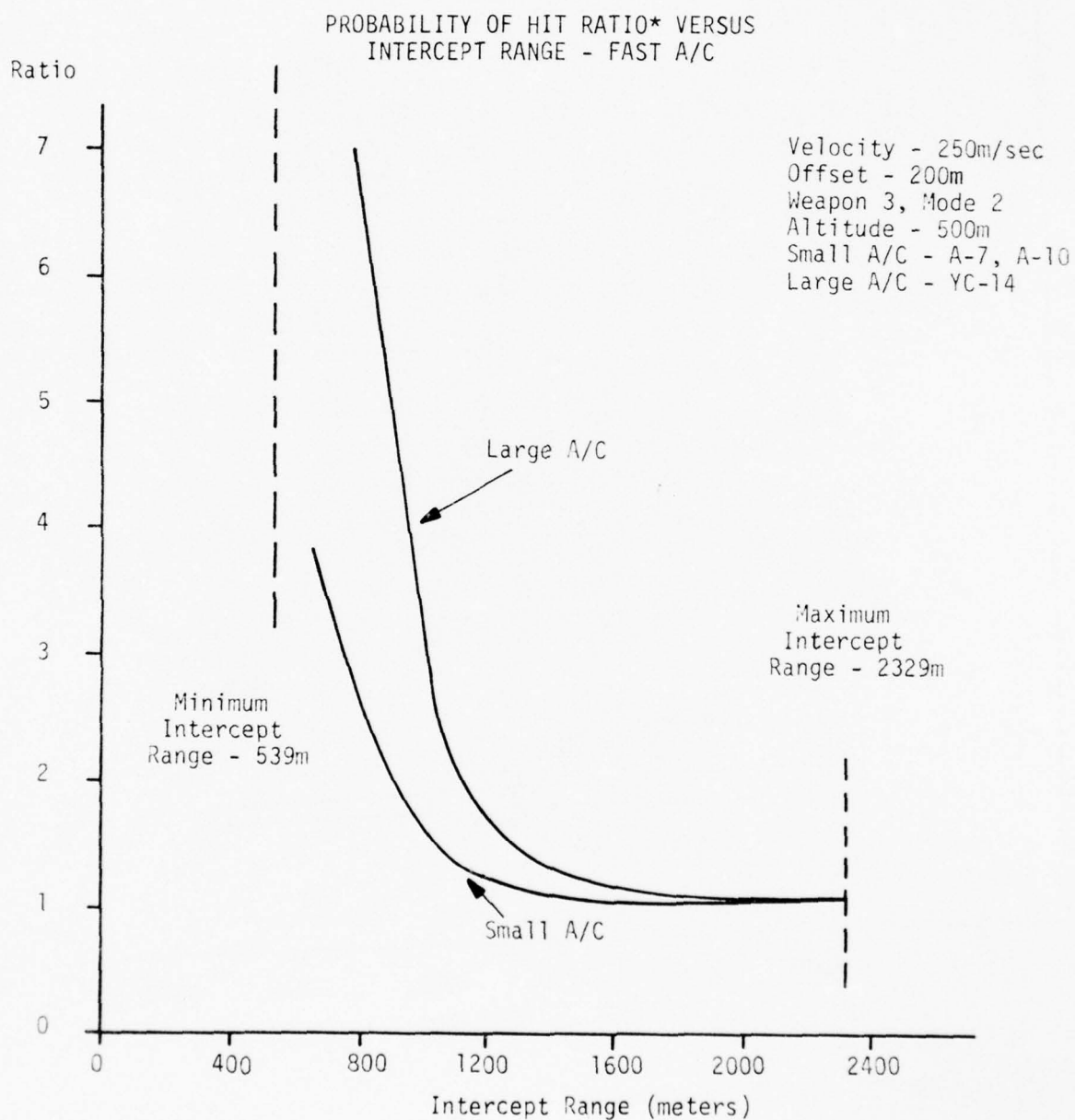
FIGURE A-9

PROBABILITY OF HIT RATIO* VERSUS
INTERCEPT RANGE - SLOW A/C



*Ratio of P_H (centroid) to P_H (extremity)

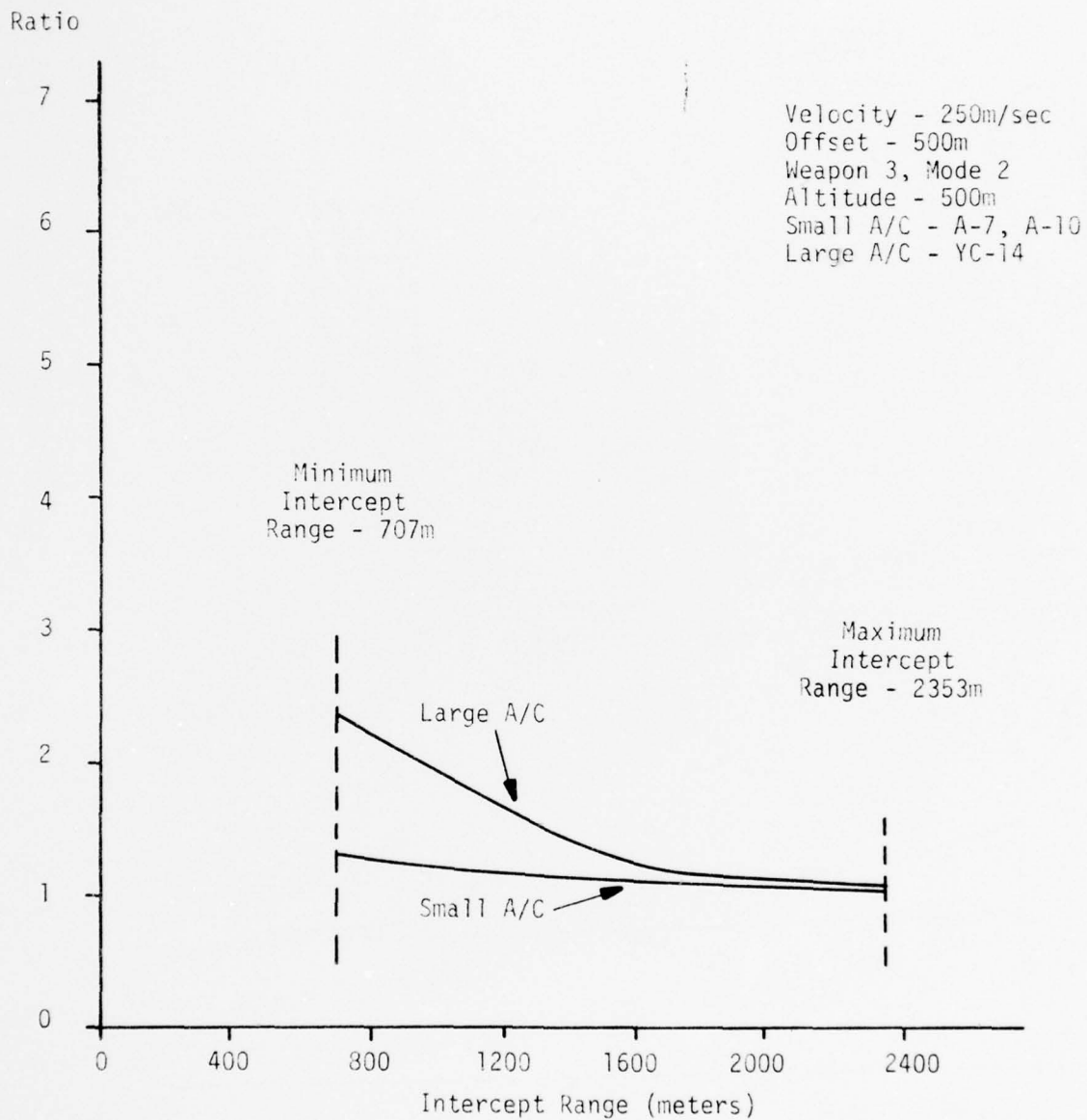
FIGURE A-10



*Ratio of P_H (centroid) to P_H (extremity)

FIGURE A-11

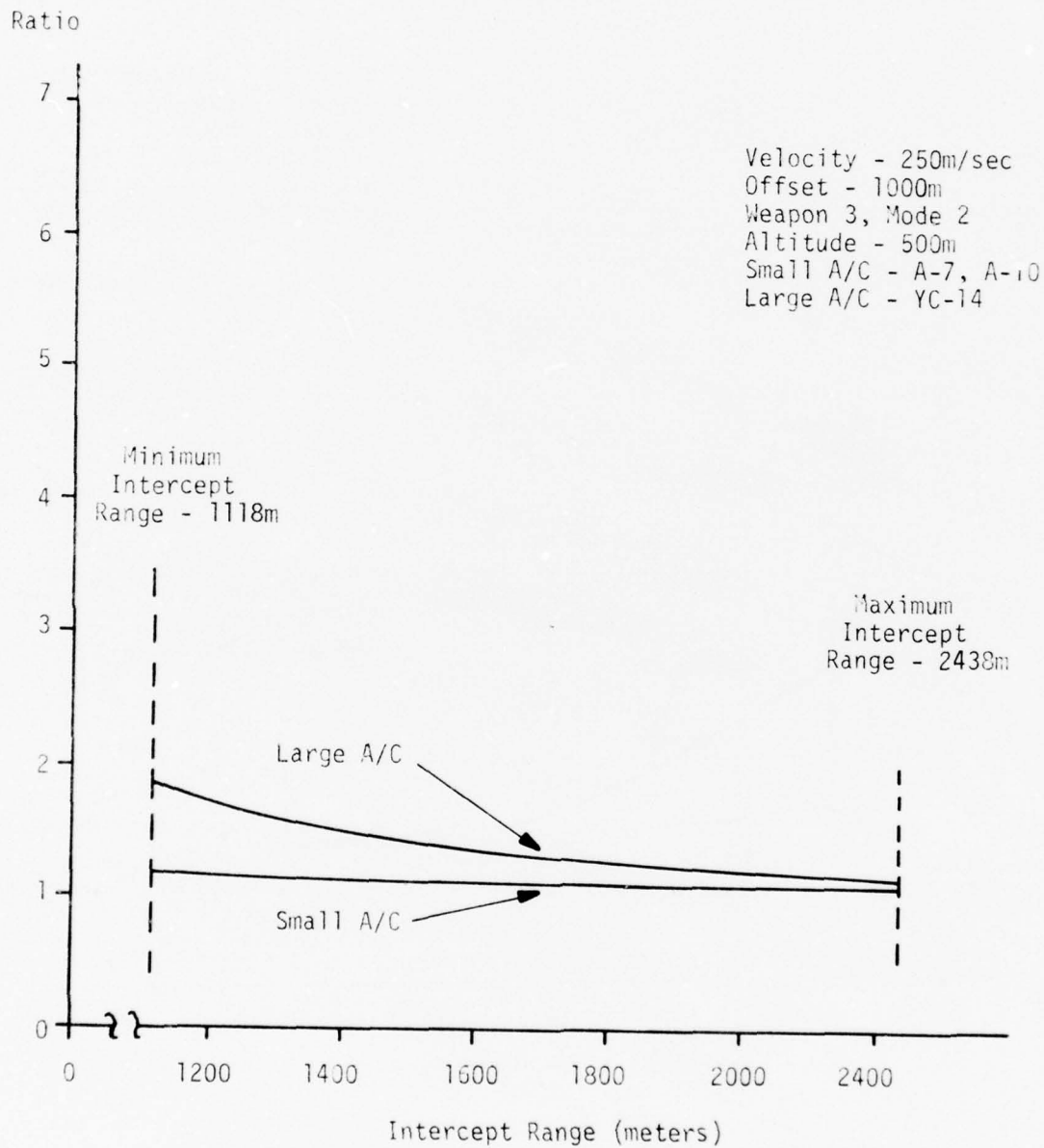
PROBABILITY OF HIT RATIO* VERSUS
INTERCEPT RANGE - FAST A/C



*Ratio of P_H (centroid) to P_H (extremity)

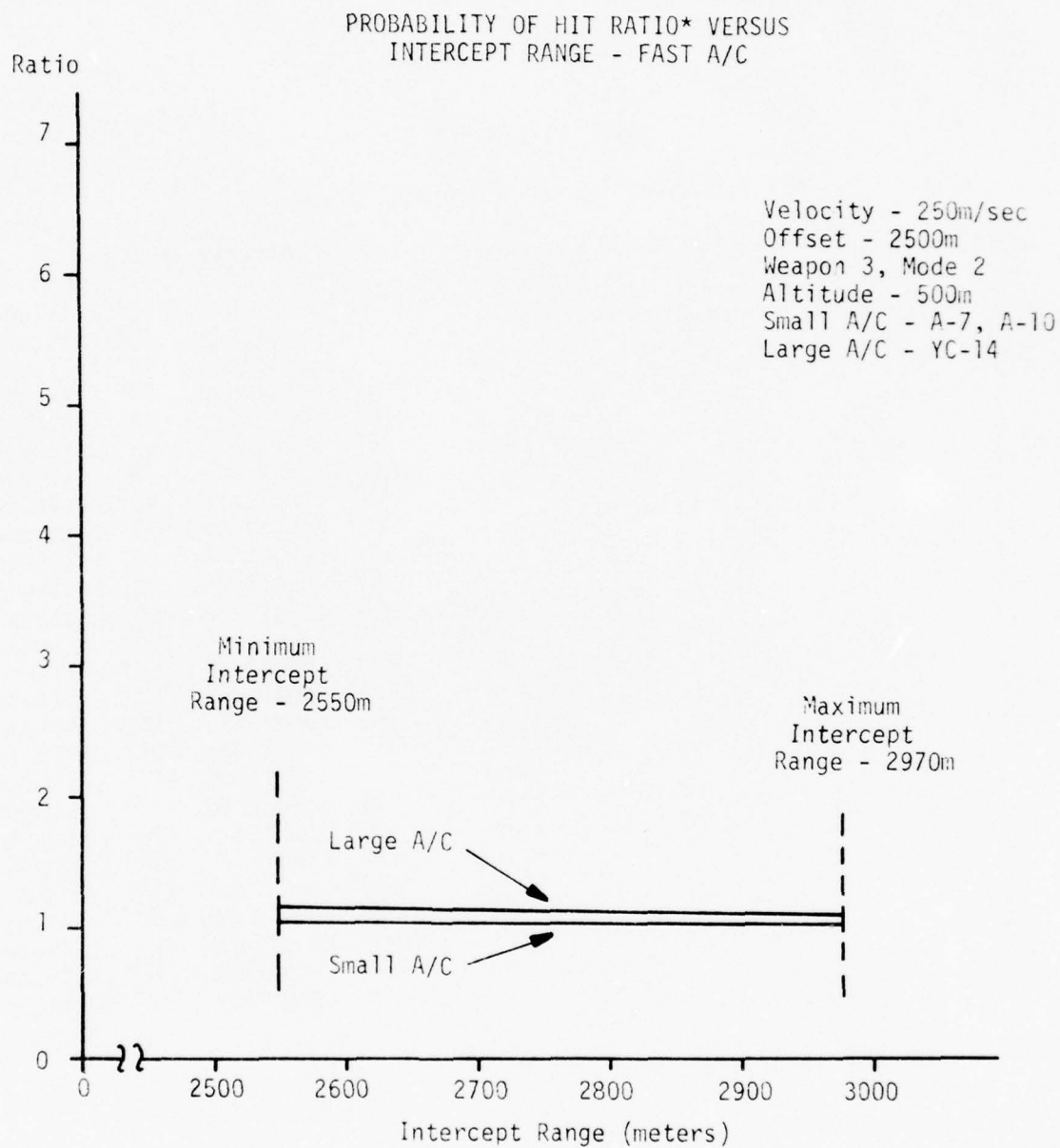
FIGURE A-12

PROBABILITY OF HIT RATIO* VERSUS
INTERCEPT RANGE - FAST A/C



*Ratio of P_H (centroid) to P_H (extremity)

FIGURE A-13



*Ratio of P_H (centroid) to P_H (extremity)

FIGURE A-14

TABLE A-1

A-7 Presented Areas - 26 Views

| <u>View</u> | <u>Presented Area* (A_p, sq. m.)</u> | <u>Aircraft View</u> |
|-------------|---|-------------------------------|
| 1 | 55.76 | 0° Longitude, 0° Latitude |
| 2 | 41.86 | 0° Longitude, 45° Latitude |
| 3 | 46.97 | 45° Longitude, 45° Latitude |
| 4 | 48.82 | 90° Longitude, 45° Latitude |
| 5 | 45.35 | 135° Longitude, 45° Latitude |
| 6 | 39.19 | 180° Longitude, 45° Latitude |
| 7 | 45.35 | 225° Longitude, 45° Latitude |
| 8 | 48.85 | 270° Longitude, 45° Latitude |
| 9 | 46.91 | 315° Longitude, 45° Latitude |
| 10 | 7.04 | 0° Longitude, 90° Latitude |
| 11 | 23.28 | 45° Longitude, 90° Latitude |
| 12 | 31.55 | 90° Longitude, 90° Latitude |
| 13 | 23.28 | 135° Longitude, 90° Latitude |
| 14 | 7.04 | 180° Longitude, 90° Latitude |
| 15 | 23.28 | 225° Longitude, 90° Latitude |
| 16 | 31.55 | 270° Longitude, 90° Latitude |
| 17 | 23.28 | 315° Longitude, 90° Latitude |
| 18 | 39.19 | 0° Longitude, 135° Latitude |
| 19 | 45.35 | 45° Longitude, 135° Latitude |
| 20 | 48.85 | 90° Longitude, 135° Latitude |
| 21 | 46.91 | 135° Longitude, 135° Latitude |
| 22 | 41.86 | 180° Longitude, 135° Latitude |
| 23 | 46.97 | 225° Longitude, 135° Latitude |
| 24 | 43.82 | 270° Longitude, 135° Latitude |
| 25 | 45.35 | 315° Longitude, 135° Latitude |
| 26 | 55.76 | 0° Longitude, 180° Latitude |

* Same for all velocities

TABLE A-2

DATA POINTS FOR GRAPHS OF RATIO* VERSUS INTERCEPT RANGE

Weapon 2, Mode 1: Velocity=50m/sec: Offset=100m: Altitude=75m

| Intercept Range | Standard Deviation | | Bias | | 1'/h' | Small A/C | | Large A/C | |
|--------------------|--------------------|------|---------|---------|-------|------------|--------|------------|--------|
| | Sf1 | Sf2 | f1 bias | f2 bias | | Exposed Ap | Ratio* | Exposed Ap | Ratio* |
| 219 | 2.9 | 2.9 | 0.5 | 0.9 | 2.0 | 30.6 | 3.13 | 122 | 45.4 |
| 329 | 3.4 | 3.4 | 1.6 | 1.3 | 1.2 | 23.0 | 1.92 | 92 | 6.65 |
| 391 | 3.8 | 3.7 | 2.6 | 0.8 | 1.0 | 19.1 | 1.75 | 76 | 4.27 |
| 446 | 4.3 | 4.1 | 2.6 | 1.0 | 1.2 | 17.6 | 1.45 | 70 | 2.56 |
| 501 | 4.8 | 4.5 | 2.5 | 1.0 | 0.7 | 16.5 | 1.30 | 66 | 2.26 |
| 609 | 5.8 | 5.4 | 2.5 | 1.1 | 0.5 | 14.8 | 1.25 | 59 | 1.97 |
| 703 | 6.7 | 6.2 | 2.6 | 1.2 | 0.4 | 13.8 | 1.21 | 55 | 1.81 |
| 812 | 7.8 | 7.1 | 2.6 | 1.3 | 0.4 | 12.9 | 1.19 | 52 | 1.49 |
| 1014 | 9.9 | 8.9 | 2.7 | 1.4 | 0.2 | 11.7 | 1.15 | 47 | 1.53 |
| 1215 | 12.1 | 10.7 | 2.8 | 1.5 | 0.2 | 10.9 | 1.12 | 44 | 1.44 |

*Ratio of Probability of Hit at Centroid to Probability of Hit at Extremity

TABLE A-3

DATA POINTS FOR GRAPHS OF RATIO* VERSUS INTERCEPT RANGE

Weapon 2, Mode 1: Velocity=50m/sec: Offset=200m: Altitude=75m

| Intercept Range | Standard Deviation | | Bias | | 1'/h' | Small A/C | | Large A/C | |
|--------------------|--------------------|-----------------|---------|---------|-------|------------|--------|------------|--------|
| | S _{f1} | S _{f2} | f1 bias | f2 bias | | Exposed Ap | Ratio* | Exposed Ap | Ratio* |
| 215 | 4.1 | 1.8 | 1.4 | 0.3 | 4.8 | 39.2 | 7.11 | 157 | 809 |
| 327 | 4.1 | 3.3 | 4.2 | 0.4 | 2.7 | 26.1 | 4.87 | 104 | 68.0 |
| 444 | 4.8 | 4.1 | 4.4 | 0.7 | 2.0 | 21.9 | 2.38 | 88 | 9.03 |
| 512 | 5.3 | 4.6 | 4.5 | 0.8 | 1.6 | 20.0 | 1.83 | 80 | 4.48 |
| 598 | 6.1 | 5.3 | 4.7 | 0.9 | 1.3 | 18.1 | 1.48 | 72 | 2.56 |
| 703 | 7.1 | 6.2 | 4.8 | 1.0 | 1.0 | 16.5 | 1.27 | 66 | 1.76 |
| 794 | 7.9 | 7.0 | 4.9 | 1.1 | 0.9 | 15.4 | 1.12 | 62 | 1.49 |
| 901 | 9.0 | 7.9 | 5.1 | 1.2 | 0.7 | 14.4 | 1.13 | 58 | 1.31 |
| 1010 | 10.1 | 8.9 | 5.2 | 1.3 | 0.6 | 13.6 | 1.09 | 54 | 1.24 |
| 1100 | 11.1 | 9.7 | 5.4 | 1.4 | 0.5 | 13.0 | 1.07 | 52 | 1.16 |
| 1440 | 15.0 | 12.8 | 6.0 | 1.6 | 0.4 | 11.6 | 1.05 | 46 | 1.17 |

*Ratio of Probability of Hit at Centroid to Probability of Hit at Extremity

TABLE A-4

DATA POINTS FOR GRAPHS OF RATIO* VERSUS INTERCEPT RANGE

Weapon 2, Mode 1: Velocity=50m/sec: Offset=500m: Altitude=75m

| Intercept Range | Standard Deviation | | Bias | | 1'/h' | Small A/C | | Large A/C | |
|--------------------|--------------------|-----------------|---------|---------|-------|------------|--------|------------|--------|
| | S _{f1} | S _{f2} | f1 bias | f2 bias | | Exposed Ap | Ratio* | Exposed Ap | Ratio* |
| 506 | 6.4 | 4.7 | 1.0 | 0.1 | 5.4 | 34.5 | 2.09 | 138 | 13.8 |
| 577 | 6.9 | 5.4 | 4.3 | 0.1 | 5.0 | 29.0 | 2.51 | 116 | 13.4 |
| 618 | 7.4 | 5.8 | 5.2 | 0.2 | 4.5 | 27.7 | 2.27 | 111 | 9.13 |
| 653 | 7.9 | 6.2 | 6.1 | 0.2 | 4.2 | 26.9 | 2.10 | 108 | 6.95 |
| 704 | 8.6 | 6.6 | 7.0 | 0.3 | 3.8 | 25.6 | 1.88 | 102 | 4.88 |
| 746 ▲ | 9.0 | 7.0 | 7.6 | 0.4 | 3.6 | 24.4 | 1.77 | 98 | 4.07 |
| 848 | 10.1 | 7.9 | 8.9 | 0.6 | 3.0 | 22.0 | 1.55 | 88 | 2.83 |
| 1003 | 11.7 | 9.3 | 10.4 | 0.8 | 2.4 | 19.5 | 1.36 | 78 | 2.01 |
| 1184 | 13.6 | 10.9 | 11.8 | 1.0 | 2.0 | 17.5 | 1.23 | 70 | 1.59 |
| 1402 | 16.1 | 12.8 | 13.2 | 1.2 | 1.5 | 15.8 | 1.15 | 63 | 1.35 |

* Ratio of Probability of Hit at Centroid to Probability of Hit at Extremity

TABLE A-5
DATA POINTS FOR GRAPHS OF RATIO* VERSUS INTERCEPT RANGE

Weapon 2, Mode 1: Velocity=250m/sec: Offset=100m: Altitude=500m

| Intercept Range | Standard Deviation | | Bias | | 1'/'h' | Small A/C | | Large A/C | |
|--------------------|--------------------|-----------------|---------|---------|--------|------------|--------|------------|--------|
| | S _{f1} | S _{f2} | f1 bias | f2 bias | | Exposed Ap | Ratio* | Exposed Ap | Ratio* |
| 548 | 51.5 | 36.3 | 17.3 | 7.9 | 3.7 | 43.9 | 1.05 | 176 | 1.12 |
| 1302 | 52.6 | 48.6 | 41.1 | 12.5 | 1.5 | 19.6 | 1.04 | 78 | 1.09 |

*Ratio of Probability of Hit at Centroid to Probability of Hit at Extremity

TABLE A-6
DATA POINTS FOR GRAPHS OF RATIO* VERSUS INTERCEPT RANGE

Weapon 2, Mode 1: Velocity=250m/sec: Offset=200m: Altitude=500m

| Intercept Range | Standard Deviation | | Bias | | 1'/h' | Small A/C | | Large A/C | |
|--------------------|--------------------|-----------------|---------|---------|-------|------------|--------|------------|--------|
| | S _{f1} | S _{f2} | f1 bias | f2 bias | | Exposed Ap | Ratio* | Exposed Ap | Ratio* |
| 539 | 62.4 | 27.5 | 28.4 | 11.9 | 3.8 | 49.6 | 1.06 | 198 | 1.13 |
| 1310 | 52.9 | 50.6 | 39.5 | 24.9 | 1.6 | 20.5 | 1.04 | 82 | 1.09 |

*Ratio of Probability of Hit at Centroid to Probability Hit at Extremity

TABLE A-7

DATA POINTS FOR GRAPHS OF RATIO* VERSUS INTERCEPT RANGE

Weapon 2, Mode 1: Velocity = 250m/sec: Offset = 500m: Altitude = 500m

| Intercept Range | Standard Deviation | | Bias | | 1'/h' | Small A/C | | Large A/C | |
|--------------------|--------------------|-----------------|---------|---------|-------|------------|---------|------------|--------|
| | S _{f1} | S _{f2} | f1 bias | f2 bias | | Exposed Ap | Ratio * | Exposed Ap | Ratio* |
| 709 | 46.6 | 26.9 | 29.8 | 5.0 | 4.0 | 46.4 | 1.11 | 186 | 1.26 |
| 1014 | 55.4 | 45.0 | 54.5 | 18.9 | 3.1 | 29.5 | 1.09 | 118 | 1.20 |
| 1298 | 61.3 | 52.9 | 60.5 | 30.1 | 2.4 | 23.7 | 1.06 | 95 | 1.14 |

*Ratio of Probability of Hit at Centroid to Probability of Hit at Extremity

TABLE A-8
DATA POINTS FOR GRAPHS OF RATIO* VERSUS INTERCEPT RANGE

Weapon 3, Mode 2: Velocity=50m/sec: Offset=200m: Altitude=75m

| Intercept Range | Standard Deviation | | Bias | | 1'/h' | Small A/C | | Large A/C | |
|--------------------|--------------------|-----------------|---------|---------|-------|------------|--------|------------|--------|
| | S _{f1} | S _{f2} | f1 bias | f2 bias | | Exposed Ap | Ratio* | Exposed Ap | Ratio* |
| 214 | 4.0 | 1.6 | 2.2 | 0.2 | 4.8 | 39.2 | 11.10 | 157 | 2250 |
| 351 | 4.1 | 3.1 | 4.4 | 0.4 | 2.7 | 25.8 | 5.00 | 103 | 70.2 |
| 381 | 2.7 | 2.7 | 0.0 | 0.4 | 2.4 | 24.1 | 2.75 | 96 | 57.0 |
| 406 | 2.9 | 2.8 | 0.1 | 0.4 | 2.3 | 23.0 | 2.26 | 92 | 24.0 |
| 480 | 3.4 | 3.3 | 0.1 | 0.4 | 1.8 | 20.5 | 1.54 | 81 | 5.27 |
| 505 | 3.6 | 3.5 | 0.1 | 0.4 | 1.7 | 19.9 | 1.41 | 79 | 3.81 |
| 599 | 4.4 | 4.2 | 0.1 | 0.3 | 1.3 | 17.8 | 1.20 | 71 | 2.02 |
| 803 | 5.6 | 5.6 | 0.1 | 0.2 | 0.9 | 15.1 | 1.09 | 60 | 1.35 |
| 1001 | 7.0 | 7.0 | 0.1 | 0.2 | 0.6 | 13.5 | 1.07 | 54 | 1.27 |
| 1098 | 7.7 | 7.6 | 0.1 | 0.2 | 0.6 | 12.9 | 1.06 | 52 | 1.24 |
| 1207 | 8.5 | 8.4 | 0.1 | 0.1 | .5 | 12.3 | 1.05 | 49 | 1.21 |
| 1807 | 12.7 | 12.6 | 0.1 | 0.1 | .2 | 10.5 | 1.04 | 42 | 1.15 |

*Ratio of Probability of Hit at Centroid to Probability of Hit at Extremity

TABLE A-9
DATA POINTS FOR GRAPHS OF RATIO* VERSUS INTERCEPT RANGE

Weapon 3, Mode 2: Velocity=50m/sec: Offset=500m: Altitude=75m

| Intercept Range | Standard Deviation | | Bias | | 1'/h' | Small A/C | | Large A/C | |
|--------------------|--------------------|------|---------|---------|-------|------------|--------|------------|--------|
| | Sf1 | Sf2 | f1 bias | f2 bias | | Exposed Ap | Ratio* | Exposed Ap | Ratio* |
| 506 | 3.9 | 3.5 | .8 | .1 | 5.5 | 34.2 | 6.67 | 173 | 974 |
| 560 | 4.1 | 3.9 | .5 | .1 | 5.2 | 29.5 | 3.74 | 118 | 137 |
| 605 | 4.4 | 4.2 | .5 | .1 | 4.7 | 28.0 | 2.70 | 112 | 40 |
| 650 | 4.7 | 4.5 | .4 | .2 | 4.2 | 26.8 | 2.09 | 107 | 15.9 |
| 700 | 5.0 | 4.9 | .4 | .2 | 3.8 | 25.4 | 1.77 | 102 | 8.32 |
| 755 | 5.4 | 5.3 | .4 | .2 | 3.5 | 23.9 | 1.53 | 95 | 4.80 |
| 803 | 5.7 | 5.6 | .4 | .2 | 3.3 | 22.7 | 1.40 | 91 | 3.50 |
| 1005 | 7.1 | 7.0 | .3 | .1 | 2.5 | 19.2 | 1.15 | 77 | 1.67 |
| 1201 | 8.5 | 8.4 | .2 | .1 | 2.0 | 17.1 | 1.07 | 68 | 1.28 |
| 1402 | 9.9 | 9.8 | .3 | .1 | 1.6 | 15.6 | 1.04 | 62 | 1.15 |
| 1605 | 11.3 | 11.2 | .3 | .1 | 1.3 | 14.4 | 1.02 | 58 | 1.09 |

*Ratio of Probability of Hit at Centroid to Probability of Hit at Extremity

TABLE A-10

DATA POINTS FOR GRAPHS OF RATIO* VERSUS INTERCEPT RANGE

Weapon 3, Mode 2: Velocity=50m/sec: Offset=1000m: Altitude=75m

| Intercept Range | Standard Deviation | | Bias | | 1'/h' | Small A/C | | Large A/C | |
|--------------------|--------------------|-----------------|---------|---------|-------|------------|--------|------------|--------|
| | S _{f1} | S _{f2} | f1 bias | f2 bias | | Exposed Ap | Ratio* | Exposed Ap | Ratio* |
| 1003 | 7.3 | 7.0 | 0.8 | 0.0 | 5.8 | 32.3 | 1.72 | 129 | 7.15 |
| 1103 | 7.9 | 7.7 | 0.6 | 0.0 | 5.6 | 27.8 | 1.45 | 111 | 3.90 |
| 1204 | 8.6 | 8.4 | 0.6 | 0.1 | 5.0 | 26.1 | 1.31 | 104 | 2.65 |
| 1401 | 10.0 | 9.8 | 0.5 | 0.1 | 4.1 | 23.4 | 1.16 | 94 | 1.70 |
| 1604 | 11.4 | 11.2 | 0.5 | 0.1 | 3.5 | 20.8 | 1.09 | 83 | 1.37 |
| 1802 | 12.8 | 12.6 | 0.4 | 0.1 | 3.1 | 19.0 | 1.06 | 76 | 1.22 |
| .. 2005 | 14.3 | 14.0 | 0.5 | 0.1 | 2.7 | 17.5 | 1.04 | 70 | 1.14 |

*Ratio of Probability of Hit at Centroid to Probability of Hit at Extremity

TABLE A-11

DATA POINTS FOR GRAPHS OF RATIO* VERSUS INTERCEPT RANGE

Weapon 3, Mode 2: Velocity=50m/sec: Offset=2500m: Altitude=75m

| Intercept Range | Standard Deviation | | Bias | | 1'/h' | Small A/C | | Large A/C | |
|--------------------|--------------------|-----------------|---------|---------|-------|------------|--------|------------|--------|
| | S _{f1} | S _{f2} | f1 bias | f2 bias | | Exposed Ap | Ratio* | Exposed Ap | Ratio* |
| 2501 | 19.0 | 17.5 | 0.8 | 0.0 | 6.2 | 30.3 | 1.08 | 121 | 1.34 |
| 2601 | 19.6 | 18.2 | 0.7 | 0.0 | 6.3 | 27.5 | 1.07 | 110 | 1.28 |
| 2801 | 20.9 | 19.7 | 0.8 | 0.0 | 5.9 | 25.5 | 1.06 | 102 | 1.21 |
| 2982 | 22.1 | 21.0 | 0.8 | 0.0 | 5.4 | 24.4 | 1.04 | 97 | 1.17 |

*Ratio of Probability of Hit at Centroid to Probability of Hit at Extremity.

TABLE A-12

DATA POINTS FOR GRAPHS OF RATIO* VERSUS INTERCEPT RANGE

Weapon 3, Mode 2: Velocity=250m/sec: Offset=200m: Altitude=500m

| Intercept Range | Standard Deviation | | Bias | | 1'/h' | Small A/C | | Large A/C | |
|--------------------|--------------------|-----------------|---------|---------|-------|------------|--------|------------|--------|
| | S _{f1} | S _{f2} | f1 bias | f2 bias | | Exposed Ap | Ratio* | Exposed Ap | Ratio* |
| 656 | 6.7 | 6.5 | 8.0 | 9.2 | 3.5 | 36.4 | 3.87 | 146 | 30.3 |
| 818 | 7.3 | 6.7 | 8.7 | 2.5 | 2.8 | 28.9 | 2.53 | 115 | 9.36 |
| 1028 | 8.6 | 8.2 | 6.4 | 2.0 | 2.2 | 23.4 | 1.49 | 94 | 2.64 |
| 1114 | 10.0 | 9.8 | 5.1 | 2.0 | 1.8 | 20.4 | 1.22 | 81 | 1.64 |
| 1400 | 11.6 | 11.4 | 4.1 | 1.9 | 1.5 | 18.2 | 1.11 | 73 | 1.30 |
| 1601 | 13.4 | 13.2 | 3.8 | 1.5 | 1.3 | 16.4 | 1.07 | 65 | 1.17 |
| 1805 | 15.3 | 15.1 | 3.6 | 1.4 | 1.1 | 15.0 | 1.04 | 60 | 1.10 |
| 2003 | 17.3 | 17.1 | 3.5 | 1.3 | 1.0 | 13.9 | 1.03 | 56 | 1.07 |
| 2329 | 20.7 | 20.5 | 4.2 | 1.8 | 0.8 | 12.6 | 1.02 | 50 | 1.03 |

*Ratio of Probability of Hit at Centroid to Probability of Hit at Extremity

TABLE A-13

DATA POINTS FOR GRAPHS OF RATIO* VERSUS INTERCEPT RANGE

Weapon 3, Mode 2: Velocity=250m/sec: Offset=500m: Altitude=500m

| Intercept Range | Standard Deviation | | Bias | | 1'/h' | Small A/C | | Large A/C | |
|--------------------|--------------------|-----------------|---------|---------|-------|------------|--------|------------|--------|
| | S _{f1} | S _{f2} | f1 bias | f2 bias | | Exposed Ap | Ratio* | Exposed Ap | Ratio* |
| 803 | 10.4 | 6.6 | 1.2 | 6.7 | 4.1 | 35.7 | 1.29 | 143 | 2.24 |
| 1020 | 9.2 | 8.3 | 1.3 | 6.2 | 3.3 | 27.7 | 1.23 | 111 | 1.97 |
| 1504 | 12.8 | 12.4 | 2.7 | 3.8 | 2.1 | 19.6 | 1.09 | 78 | 1.26 |
| 1813 | 15.7 | 15.2 | 2.7 | 2.9 | 1.7 | 16.8 | 1.04 | 67 | 1.12 |
| 2353 | 21.2 | 20.8 | 4.0 | 2.5 | 1.2 | 13.8 | 1.02 | 55 | 1.06 |

*Ratio of Probability of Hit at Centroid to Probability of Hit at Extremity

TABLE A-14
DATA POINTS FOR GRAPHS OF RATIO* VERSUS INTERCEPT RANGE

Weapon 3, Mode 2: Velocity=250m/sec: Offset=1000m: Altitude=500m

| Intercept Range | Standard Deviation | | Bias | | 1'/h' | Small A/C | | Large A/C | |
|--------------------|--------------------|-----------------|---------|---------|-------|------------|--------|------------|--------|
| | S _{f1} | S _{f2} | f1 bias | f2 bias | | Exposed Ap | Ratio* | Exposed Ap | Ratio* |
| 1201 | 13.9 | 9.8 | 2.0 | 2.5 | 5.1 | 32.2 | 1.19 | 129 | 1.74 |
| 1394 | 13.9 | 11.4 | 1.9 | 3.3 | 4.5 | 26.6 | 1.14 | 105 | 1.52 |
| 1582 | 15.0 | 13.1 | 2.2 | 3.2 | 4.0 | 23.3 | 1.10 | 93 | 1.35 |
| 1814 | 16.9 | 15.3 | 2.3 | 2.9 | 3.5 | 20.3 | 1.07 | 81 | 1.21 |
| 2438 | 23.1 | 21.7 | 5.2 | 2.5 | 2.5 | 15.7 | 1.04 | 63 | 1.10 |

*Ratio of Probability of Hit at Centroid to Probability of Hit at Extremity

TABLE A-15
DATA POINTS FOR GRAPHS OF RATIO* VERSUS INTERCEPT RANGE

Weapon 3, Mode 2: Velocity=250 m/sec: Offset=2500m: Altitude=500m

| Intercept Range | Standard Deviation | | Bias | | 1'/h' | Small A/C | | Large A/C | |
|--------------------|--------------------|------|---------|---------|-------|------------|--------|------------|--------|
| | Sf1 | Sf2 | f1 bias | f2 bias | | Exposed Ap | Ratio* | Exposed Ap | Ratio* |
| 2550 | 44.1 | 22.9 | 10.2 | 0.3 | 6.8 | 27.5 | 1.05 | 110 | 1.13 |
| 2970 | 37.4 | 27.9 | 5.5 | 1.1 | 6.8 | 20.3 | 1.04 | 81 | 1.10 |

*Ratio of Probability of Hit at Centroid to Probability Hit at Extremity

APPENDIX B

Determination of f1-f2 coordinates for vulnerable components
not at the aircraft's centroid.

METHODOLOGY FOR EXACT POSITION OF VULNERABLE COMPONENT

The technique for determining the exact position of a vulnerable component (not at the aircraft's centroid) in the f1-f2 geometric plane as shown in reference (2) is summarized below.

1. The coordinates (VCX, VCY, VCZ) of the vulnerable component are defined in the Aircraft Coordinate System. This coordinate system is shown in Figure B-1. In this system the centroid has the coordinates (0, 0, 0).

2. The coordinates of the vulnerable component are then transformed into the gun-centered system. The M inverse matrix (M^{-1}) is needed to transform the aircraft system vectors into the gun-centered system. The M matrix which is used for the reverse transformation is defined in equation 2.187 on page 2-43 of reference (1), Volume I and is shown below.

$$\begin{bmatrix} (\cos\tilde{\alpha} \cos\tilde{\beta}) & (\cos\tilde{\alpha} \sin\tilde{\beta}) & (\sin\tilde{\alpha}) \\ (-\cos\tilde{\psi} \sin\tilde{\beta} - \sin\tilde{\psi} \sin\tilde{\alpha} \cos\tilde{\beta}) & (\cos\tilde{\psi} \cos\tilde{\beta} - \sin\tilde{\psi} \sin\tilde{\alpha} \sin\tilde{\beta}) & (\sin\tilde{\psi} \cos\tilde{\alpha}) \\ (\sin\tilde{\beta} \sin\tilde{\psi} - \cos\tilde{\psi} \sin\tilde{\alpha} \cos\tilde{\beta}) & (-\sin\tilde{\psi} \cos\tilde{\beta} - \cos\tilde{\psi} \sin\tilde{\alpha} \sin\tilde{\beta}) & (\cos\tilde{\psi} \cos\tilde{\alpha}) \end{bmatrix}$$

The M matrix is also listed on page 33 of reference (2), where the elements are shown as B(1,1) through B(3,3).

The M inverse (M^{-1}) is used to transform the position vector of the vulnerable component from the aircraft coordinate system into a gun-centered correction vector which will be added to the position of the centroid in the gun-centered system.

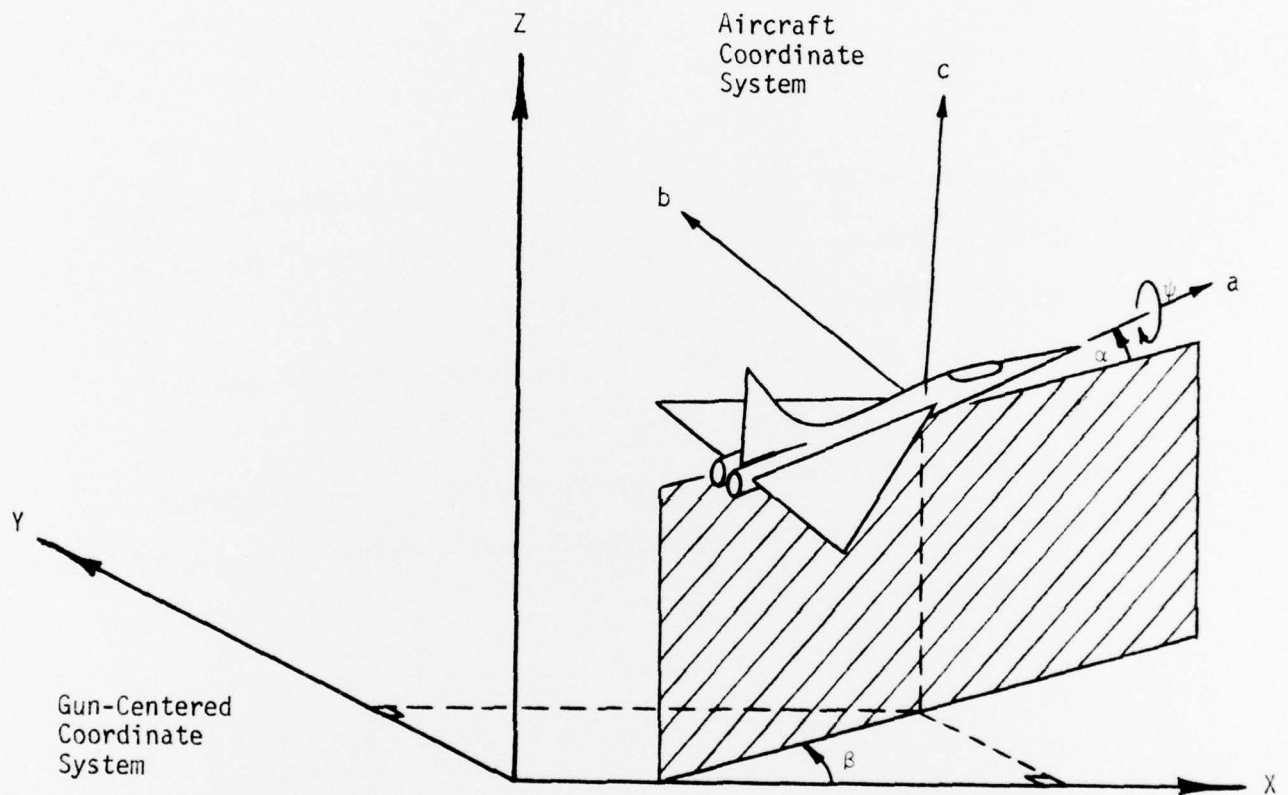


FIGURE B-1

AIRCRAFT COORDINATE SYSTEM RELATIVE
TO THE GUN-CENTERED COORDINATE SYSTEMS

Distances in x, y, z
from aim point

Distances in a, b, c
from aim point

$$\begin{bmatrix} \text{VCXM (X)} \\ \text{VCYM (Y)} \\ \text{VCZM (Z)} \end{bmatrix} = [M]^{-1} \begin{bmatrix} \text{VCX (a)} \\ \text{VCY (b)} \\ \text{VCZ (c)} \end{bmatrix}$$

Coordinates of the centroid are (XA, YA, ZA). Therefore, coordinates of the vulnerable component in the gun-centered coordinate system are (XA + VCXM, YA + VCYM, ZA + VCZM).

3. The coordinates of the vulnerable component are then transformed into the aim system.

The gun centered coordinates are transformed into aim system coordinates by equation 2.177, page 2-39 of reference (1), Volume I, as shown below.

$$\begin{bmatrix} X' \\ Y' \end{bmatrix} = \begin{bmatrix} \sin \bar{\theta} & -\cos \bar{\theta} & 0 \\ -\sin \bar{\phi} \cos \bar{\theta} & -\sin \bar{\phi} \sin \bar{\theta} & \cos \bar{\phi} \end{bmatrix} \begin{bmatrix} XA + VCXM \\ YA + VCYM \\ ZA + VCZM \end{bmatrix}$$

Aim system
Coordinates

Gun Centered
Coordinates

4. Then the coordinates of the vulnerable component are transformed into the Final System.

The aim system coordinates (X', Y') are transformed into the final system coordinates (f1 bias, f2 bias) by equation 2.178, page 2-39 of Volume I of reference (1) as shown below.

$$\begin{bmatrix} f1 \text{ bias} \\ f2 \text{ bias} \end{bmatrix} = \begin{bmatrix} \cos \eta & \sin \eta \\ -\sin \eta & \cos \eta \end{bmatrix} \begin{bmatrix} X' \\ Y' \end{bmatrix}$$

Final System
Coordinates
Gun-Centered
Coordinates

Thus, the final system coordinates of the vulnerable component (not at the centroid) are (f1 bias, f2 bias).

DISTRIBUTION LIST

No. of Copies

Commander
Naval Sea Systems Command
Washington, DC 20360
Attention: SEA-6543C - Mr. Frank W. Sieve 1

Commander
Naval Weapons Center
China Lake, CA 93555
Attention: Code 408 - Mr. H. W. Drake 1

Commanding General
Ballistics Research Laboratory
Aberdeen Proving Ground
Aberdeen, MD 21005
Attention: AMXBR-VL - Mr. D. W. Mowrer 1

Commander
Air Force Flight Dynamics Laboratory
Wright-Patterson AFB, OH 45433
Attention: PTS - Mr. D. W. Voys 1

Commander
ASD
Wright-Patterson AFB, OH 45433
Attention: ASD/XRHD - Mr. B. Bennett 1
ASD/ENY - Mr. Donald J. Wallick 1

Commanding Officer
Naval Surface Weapons Center
Dahlgren, VA 22448
Attention: Code GA - Mr. T. H. McCants 1

Commander
Naval Air Development Center
Warminster, PA 18974
Attention: SAED/SDE - Mr. M. C. Mitchell 1

Commander
Air Force ATL
Eglin AFB, FL 32542
Attention: DLYV - Mr. J. A. Rutland 1
DLYW - Mr. W. D. Thomas 1

Administrator
Defense Documentation Center for Scientific
and Technical Information (DAC)
Building 5, Cameron Station
Alexandria, VA 22314 12

